Recent advances in waste-based and natural zeolitic catalytic materials for biodiesel production

Dalibor M. Marinković and Stefan M. Pavlović

University of Belgrade, Institute of Chemistry, Technology and Metallurgy, Belgrade, Serbia

Abstract

Considering the current world crisis and definite future energy challenges, biomass-to-fuel transformation is increasingly becoming important both to the policy makers and to the industry. In this perspective, the valorisation of oils and fats *via* transesterification/esterification reaction is an attractive method for producing biodiesel with qualities suitable for diesel engines. The recent interest indicated a significant shift to industrial waste valorisation as another approach for achieving process eco-efficiency. In this respect, the use of zeolite-based catalysts for the production of biofuels is reviewed here, with a special emphasis on the utilization of waste raw materials following the principles of green chemistry and sustainable development. Zeolites are interesting due to their outstanding catalytic properties, including the presence of intrinsic acid sites, simple loading of base sites, shape-selectivity, and high thermal stability. Neat zeolites or modified by the loading of active species are classified into several groups following their origin. For each group, the most relevant recent results reported in the literature are reviewed together with some critical considerations on the catalyst effectiveness, stability, reusability, and economy of synthesis. As an important part required for understanding and optimization of the biodiesel production process, the mechanisms of the reaction were discussed in detail. Finally, key perspective directions for further research studies were carefully identified and elaborated.

Keywords: zeolite; waste raw materials; fly ash; industrial waste; heterogeneous catalysis; transesterification.

Available on-line at the Journal web address: http://www.ache.org.rs/HI/

1. INTRODUCTION

In recent decades, especially in recent years, more and more attention is focused on energy consumption, energy efficiency, fossil fuel emission and depletion, as well as on alternative energy sources and uses [1]. World crises are only intensifying these issues. The world dependence on fossil fuels is still dominant, but some renewable solutions are available, while many are being intensively researched. Biofuels, such as biodiesel, are significant competitors to fossil diesel fuel, due to lower contents of CO_2, SO_2, and hydrocarbons during combustion, as well as biodegradability, high flash point, high lubricant properties, and high octane number [2,3]. Additionally, biodiesel can be used in modern internal combustion engines without modification [4]. Commercial production of biodiesel began in Austria in 1991, and for the next 15 or so years, biodiesel production was booming. It seems that after that first run, interest in biodiesel declined until recently when it became attractive again with the intensification of the world energy crisis. Current chemical technology practices of obtaining biodiesel imply the following concepts: base-catalysed transesterification (homogeneous or heterogeneous) [5-7], acid-catalysed esterification and transesterification [8,9], enzyme-catalysed transesterification [10,11], biodiesel synthesis catalysed by bifunctional heterogeneous solid catalysts [12,13], deoxygenation [14,15], and supercritical methanolysis [16,17]. Process intensification in terms of the reaction mixture treatment by microwave [18,19] and ultrasound [20,21] is also a part of the latest interest of the researchers. The modern approach in biodiesel research, however, synergistically focuses on new catalytic systems based on waste sources, the use of non-edible or waste triacylglycerol (TG) feedstock, and on advanced batch and continuous reactor systems. Such an approach is not only sustainable and environmentally friendly but also economically viable.

Nowadays, homogeneous base and acid catalysts are still used in most industrial plants for biodiesel production, despite their numerous disadvantages (demanding catalyst recovery, soap formation, difficult product purification, high corrosion, and inhibition by water) [3]. The modern concept of sustainable industrial processes strongly supports design of new catalysts based on waste materials, such as biomass fly ash, coal-fired power stations fly ash, industrial waste rich in calcium and other alkali and alkaline earth metals such as mud and slug, agricultural and animal waste, and natural sources [22]. The use of these materials has a double benefit, as economic and environmental problems of disposal and treatment of waste materials are being solved, and, on the other side, very useful and valuable catalytic materials are obtained, further utilized in obtaining biofuels. Particular attention of researchers is focused on the challenge of adaptation of the mentioned catalytic systems to produce biodiesel from waste TG sources, such as non-edible oils, waste cooking oils (WCOs), and oils with high free fatty acid (FFA) contents [23]. Also, attention is paid to the modern biodiesel production process from oils obtained from microalgae [24].

Zeolite is a crystalline aluminosilicate material with various spatial three-dimensional structures that allow the adsorption and diffusion of molecules. It can occur naturally or can be synthesized from pure chemicals, natural minerals, or waste materials. Zeolitic materials have found great interest among researchers and in the industry because of their easily tunable physical and chemical properties. Nowadays, they are successfully investigated and used as catalysts in different processes such as isomerisation, condensation and oligomerization, pyrolysis or liquefaction, hydrolysis, esterification, and transesterification [25]. Unlike many other materials that could be employed as catalysts for TGs conversions, zeolites are highly stable with the potential to resist severe reaction conditions [26]. Their structure is responsible for very high melting points (higher than 1,000 °C), so zeolites can withstand elevated reaction pressures and temperatures and are stable in air and many solvents used in catalysis. Tunable acidity/basicity and suitable structural properties of zeolitic materials account for their wide exploitation as prospective catalysts.

One of the major drawbacks of a heterogeneously catalysed transesterification process is diffusion-limited mass transport in porous materials. Furthermore, the reaction mixture molecules could be massively deposited onto the catalyst surface and cause pore-blocking, leading to a reduction in catalyst activity [27]. These issues can be resolved by using hierarchically structured zeolitic materials with double or triple porosity, *i.e.*, meso- and/or macroporosity [28]. Besides that, along with the principles of sustainable development, zeolitic materials can be obtained from waste that has an adequate ratio of constituent atoms (Al and Si), such as fly and bottom ashes generated in thermal power plants [29].

Several review papers already dealt with the use of zeolite catalysis in biofuel production [25,26,30]. Thus, the present review is focused on waste-based and natural zeolitic materials and their use as catalysts or catalyst supports in biodiesel production as a supplement to previous articles. The synthesis routes of zeolite-based catalyses will be analysed in detail, with an emphasis on the economy of synthesis, as well as on key analytical parameters of the synthesized materials. The quality of biodiesel obtained by using zeolite-based catalysts and mainly non-edible or waste oil feedstocks will be considered, as well as the stability and recyclability of the catalyst. Finally, reaction mechanisms will be discussed in detail as for optimization of the reaction conditions, it is necessary to understand what happens to the reactants and products in the course of the reaction.

2. ZEOLITES, ORIGIN, STRUCTURE

Zeolites are crystalline porous materials structured as a tetrahedral TO_4 (T = Al, Si) in different orders, resulting in 253 unique frameworks, with over 40 naturally occurring frameworks [31]. The term "zeolite" was originally addressed by the Swedish mineralogist Axel Cronstedt in the mid-eighteenth century. He observed that rapid heating of material produces huge amounts of vapour that had been previously adsorbed. Based on this observation, he called the material "zeolite", from the Greek words "zeo" and "lithos", meaning "to boil" and "stone", respectively. [32]. zeolite-specific structure, *i.e.* channel- or cage-like system, acts as a trap for molecules of specific sizes and shapes [33]. In the porous structure of zeolite a wide variety of cations can be accommodated, such as Na^+, K^+, Ca^{2+}, Mg^{2+}, and others. These cations are loosely bonded and can be easily exchanged with other ions present in the contact solution. The relationship between the contents of exchangeable cations and aluminium in the aluminosilicate framework is always (Ca + Mg + Ba + Na_2 + K_2)/Al = 1. Zeolites differ from all the other framework silicates by the presence of water molecules. The general

formula for a zeolite mineral is: $(Ca, Na_2, K_2, Ba, Sr, Mg, Cs_2, Li_2)_a[Al_2Si_{n-a}O_{2n}] \times H_2O$, where atoms in the square brackets represent the framework atoms, and the rest represents the exchangeable ions plus water [34].

Zeolitic materials can occur naturally but can be also produced industrially on a large scale. Natural zeolite groups include: analcime (pollucite and wairakite), chabazite (herschelite and willhendersonile), gismondine (amicite, garronite, and gobbinsite), heulandite (clinoptilolite), natrolite (mesolite and scolecite), harmotome (phillipsite and wellsite), and stilbite (barrerite and stellerite) [34]. An example of the structure of one of the most abundant natural zeolites mordenite, with a mineral formula of $(Ca, Na_2, K_2) Al_2Si_{10}O_{24}·7H_2O$ is presented in Figure 1.
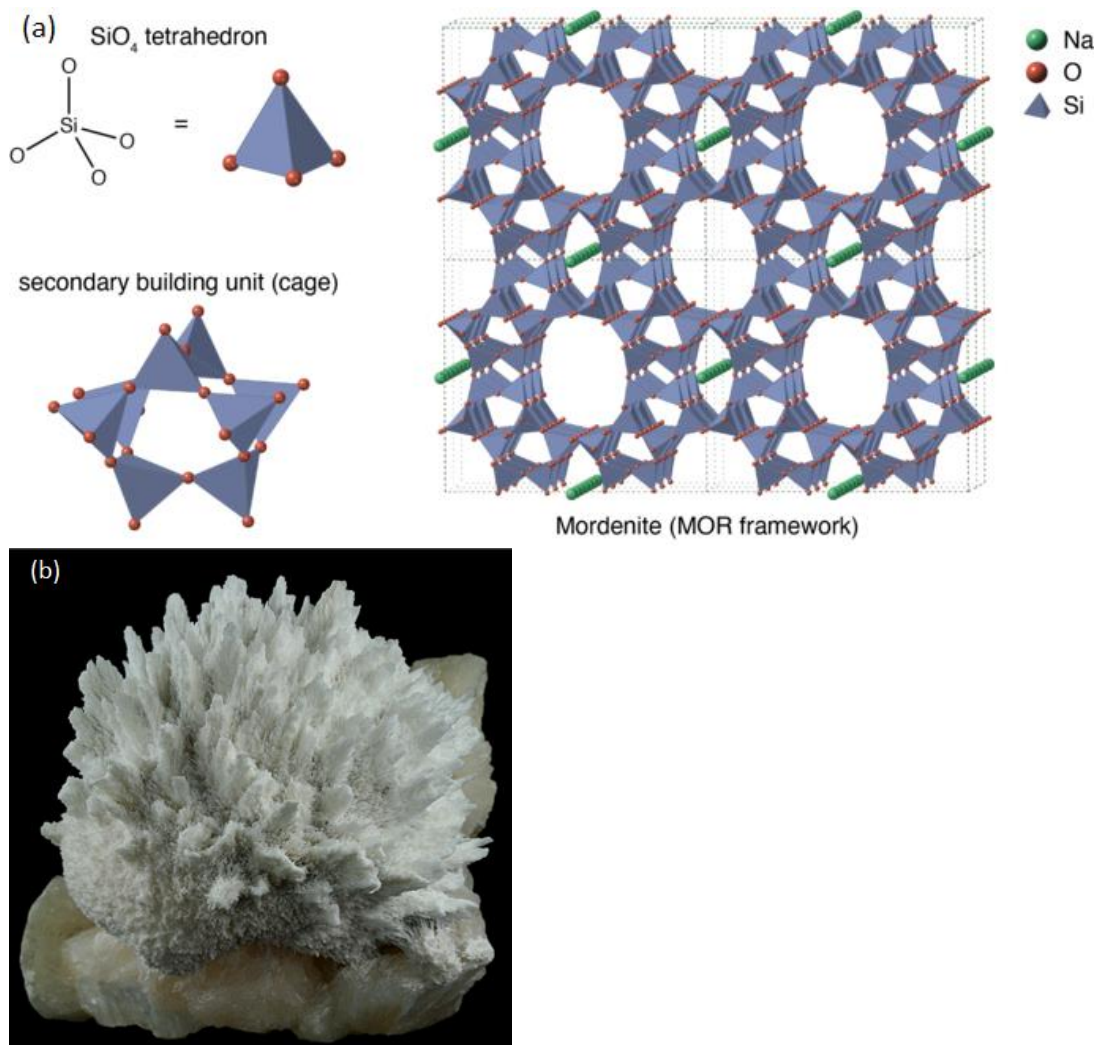

Figure 1. Typical structure (a) and appearance (Indian mine) (b) of mordenite framework [34]

Zeolite materials find application in many industrial processes, the most important being catalysis [35], adsorption [36], and separation [37]. The term „molecular sieve" related to zeolitic materials refers to the particular ability to selectively sort other molecules based on their size, due to a rather regular zeolite framework, that is the pore structure. For industrial applications synthetic zeolites are certainly more important since their structure may be more regular than that of natural ones.

The interest of researchers in biodiesel and the use of zeolitic materials in catalytic biodiesel production is increasing over the 21st century. Figure 2 shows the number of published papers indexed in the Scopus database [38,39], which have as their topic biodiesel and the use of zeolite materials in heterogeneous catalytic production of biodiesel. The number of papers shows that interest in biodiesel is significant, with about a hundred papers published annually from the beginning of the 21st century, up to about as many as 4,000 articles published annually nowadays. The attractiveness

of zeolitic materials as catalysts for biodiesel production also tends to expand. Interest in this topic was almost negligible at the beginning of the 21st century, at least according to published articles, while today there are more than 50 articles published per year (Fig. 2).
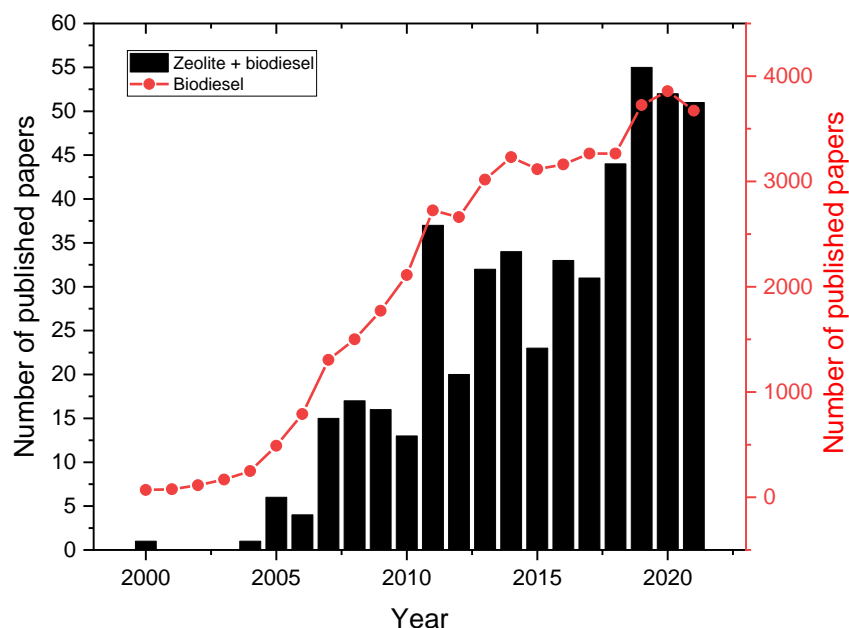

Figure 2. Number of published articles related to the use of zeolite in biodiesel production and the overall number of articles on biodiesel indexed by Scopus in the period 2000-2021 [38,39]

2. 1. Natural zeolites

Natural zeolites are conventionally obtained in open-pit mines, where the overburden is mechanically removed to excavate the ore. Common zeolite groups with similar frameworks and their main and distinctive characteristics are presented in Table 1 [34].

Natural zeolites are formed in Earth's crust in a water-abundant environment under a wide range of temperatures and, often, under low pressure. They are rarely pure and are accompanied by various contents of other minerals, such as quartz, metals, and other zeolite species. Zeolites are formed in the contact of volcanic ash, rocks, and pyroclastic materials with saline, alkaline water, deep sea sediments, shallow marine seas, hot springs, and freshwater lakes. There are several mechanisms of natural zeolite formation, and two distinctive pathways are: low-temperature (4-40 °C) and elevated-temperature origins (40-250 °C). An example of the first is phillipsite, which is formed in deep-sea sediments and needs approximately 150,000 to 10,000,000 years to crystallize. Examples of the second pathway can be the formation of different zeolitic crystals depending on the increase in temperature during the contact metamorphism process, which are as follows [34]:

mordenite-quartz → chabazite-stilbite-heulandite-gmelinite → mesolite-scolecite-natrolite-thompsonite-
-laumontite-analcime → albite-epidote-prehnite-pumpellyite → granitic intrusion

World reserves of natural zeolites have not been estimated yet. Deposits occur in many countries, but companies and states rarely publish reserves data. The United States, for example, reported combined reserves of 80 million tons in 2021, while the total U.S. reserves are likely substantially larger [41]. In 2021, the world´s annual mine production of natural zeolite was estimated at 944,000 t, which is significantly lower than a few years ago as the production of natural zeolite in 2015 was about 2.78 million tons. Major producers in 2021 (estimation) included Georgia (140,000 t), Indonesia (130,000 t), the Republic of Korea (130,000 t), Slovakia (120,000 t), Unites States (87,000 t), Cuba (53,000 t), China (52,000 t), and Turkey (50,000 t). China has significantly reduced its production, for example in 2015 it produced as much as 2 million tons of natural zeolite [41]

Table 1. Groups of zeolite types sorted by the framework [34]

Group holder	Associated types	Main characteristics
Analcime	Pollucite Wairakite	• Wide variation in chemical composition and disorder-order in the framework • Analcime contains Na • Pollucite contains Cs • Wairakite contains Ca
Chabazite	Horschelite Willhendersonite	• Wide variation in chemical composition and disorder-order in the framework • Chabasite crystals are Ca dominant, although K, Mg, and Na could be present • Chabazite and willhendersonite have the same triclinic framework and can have the same K dominant chemical composition (they differ in the amount of Si and Al)
Gismondine	Amicite Garronite Gobbinsite	• The associated members could be considered disordered gismondine or Na-K-dominant gismondine
Heulandite	Clinoptilolite	• These crystals have been divided into three sets of criteria, a gap in Si/Al mole ratio (Si/Al), a gap in Na-K-Mg-Ca-content, and a gap in the heating characteristics of the framework • Clinoptilolite is often considered as Si dominant heulandite
Natrolite	Mesolite Scolecite Tetranatrolite Gonnardite	• Natrolite, mesolite, and scolecite have a dominantly ordered framework, with different chemical composition • Natrolite, tetranatrolite, and gonnardite differ in the amount of disorder/order of Al and Si in the framework and Na and Ca content • Tetranatrolite is often considered as a Na dominant gonnardite
Harmotome	Phillipsite Wellsite	• These crystals have a single framework with a continuous chemical series ranging from K-Ca-Na-dominant in phillipsite to K-Ca-Ba-dominant in wellasite to Ba-dominant in harmotome
Stilbite	Barrerite Stellerite	• These crystals have identical morphology; the difference is in the ordering of Si/Al in the framework, and the exchangeable Ca and Na ions • Stellerite has Ca as the exchangeable cation and most of the sectors in the framework are orthorhombic • Barrerite has also an orthorhombic structure with present Na, K, and Ca • Stilbite has a wide range of Ca, Na, and K with various amounts of monoclinic, orthorhombic, and triclinic sectors in the same crystal

World reserves of natural zeolites have not been estimated yet. Deposits occur in many countries, but companies and states rarely publish reserves data. The United States, for example, reported combined reserves of 80 million tons in 2021, while the total U.S. reserves are likely substantially larger [41]. In 2021, the world´s annual mine production of natural zeolite was estimated at 944,000 t, which is significantly lower than a few years ago as the production of natural zeolite in 2015 was about 2.78 million tons. Major producers in 2021 (estimation) included Georgia (140,000 t), Indonesia (130,000 t), the Republic of Korea (130,000 t), Slovakia (120,000 t), Unites States (87,000 t), Cuba (53,000 t), China (52,000 t), and Turkey (50,000 t). China has significantly reduced its production, for example in 2015 it produced as much as 2 million tons of natural zeolite [41],
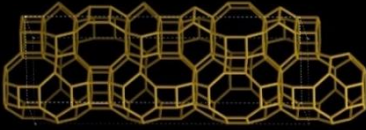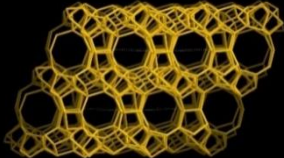
2. 2. Synthetic zeolites

In the mid-1940s, Barrer and Milton opened the story of zeolite synthesis [41] and since then, the interest in various synthesis routes of different zeolitic materials did not stop. Today, the Structure Commission within the International Zeolite Association denotes each synthesized zeolite by a three-letter code. The latest zeolite codes approved since 2020 and their frameworks are presented in Table 2 [31].

Zeolites are commonly synthesized under hydrothermal/solvothermal conditions with alkali metal ions or organic amines/ammonium ions as the structure-directing agents (SDAs) or templates. The reactive reagents usually include tetrahedral atom (Al, Si, P, *etc*.) sources, SDA, mineraliser (OH$^-$ or F$^-$), solvent, *etc*. Many synthesis parameters are crucial in the zeolite formation such as: source materials, composition, the solvent Si/Al mole ratio, SDA, crystallization temperature, pH value, and ageing/crystallization time. Due to the vast diversity of routes, there is insufficient understanding, so far, of the formation mechanism of zeolite materials. Somewhat harsh conditions of synthesis inspired many researchers to make efforts toward greener synthesis routes [41].

The published studies emphasize the use of renewable or waste feedstock, energy efficiency, safer solvents and auxiliaries, and utilization of less hazardous chemicals and synthesis conditions [28]. However, the traditional zeolite synthesis deviates to a certain extent from the principles of green chemistry.

Table 2. Newest framework types of synthetic zeolites approved by the International Zeolite Association [34]

Framework type	Cell parameters	Accessible volume fraction, %	Framework image
ANO	hexagonal	12.4	
PTO	monoclinic	9.12	
PTT	trigonal	10.38	
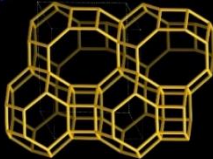
The hydrothermal or solvothermal synthesis methods commonly require high temperatures and pressures, which unequivocally increases energy consumption and raises process risks. Organic solvents are usually expensive and toxic and therefore increase costs and environmental impact. The obtained filtrates contain inorganic/organic molecules that should be recuperated and reused. Finally, the resulting precursors need to be calcined at high temperatures, which is not economically nor environmentally attractive. Researchers have therefore been making huge efforts to develop different routes to guide the process of zeolite synthesis according to the principles of green chemistry, such as: waste reusing [29], environmental and cost impact reduction, increased energy efficiency [29,42], process safety [41], *etc*. Many studies are oriented towards the rational synthesis of zeolitic materials with specific novel framework structures and functions [43].

3. ZEOLITES AS CATALYSTS

Since WWII, the development of zeolite-based catalysts has been one of the most impressive breakthroughs in the catalysis world. In the beginning, it was just the curiosity of researchers to investigate their property of adsorption and desorption of water when heated, so in the period of 1940s researchers at the Union Carbide (Linde division) synthesized zeolites A, B, and X [25]. In the following years, commercialisation of these zeolites started as gas separation adsorbents. Shortly afterwards, researchers at Union Carbide and Mobil discovered the zeolite shape selectivity and how to control it and thus, the golden age of zeolite use as catalysts began.

Different zeolite origins, structures and the resulting physical and chemical characteristics have logically resulted in the classification of zeolite-based catalysts into several groups: natural- zeolite-based catalysts, synthetic zeolite-based catalysts, and waste-based zeolitic catalysts.

3. 1. Natural zeolites as catalysts

Chemically modified natural minerals and rocks were investigated widely in the synthesis of low-cost, easily available, and environmental heterogeneous catalysts for biodiesel production [44]. Natural zeolitic materials are widely available in mines around the world and are considered relatively inexpensive [45]. This type of zeolite material is highly desirable because of the possibility to control the functionalisation of the zeolite surface by acidic or basic groups to achieve high catalytic performance and consequently high biodiesel yields. In addition, natural zeolite-based catalysts have the important advantage of avoiding the zeolite synthesis step compared to synthetic zeolite-based catalysts and waste-based zeolitic catalysts, which significantly shortens the catalyst synthesis time and lowers the energy used.

Conducted studies (Table 3) demonstrated that decoration of zeolite by nanoparticles or modification of zeolite structure by alkali or alkali earth metals/oxides resulted in catalysts of enhanced morphological properties, high surface area with good porosity, and finely dispersed numerous catalytically active sites. These catalytic materials have most often succeeded in achieving high activity and yielding FAME greater than 90 % using mild reaction conditions (Table 4).

Table 3. Review of preparation routes and characteristics of natural zeolitic catalysts

Catalyst designation and origin	Catalyst preparation	Catalyst characteristics	Ref.
KOH/clinoptilolite Clinoptilolite (Semnan, northeast of Iran)	**Impregnation** • Impregnation under constant stirring at 60 °C for 24 h • KOH/clinoptilolite ratio of 1:4 • Drying and calcination at 400 °C for 5 h	Content (XRF), %: (SiO_2) 60.6; (K_2O) 25.5; (Al_2O_3) 6.8; (Na_2O) 1.2; (Fe_2O_3) 1.1; (CaO) 1.0; (MgO) 0.65; (TiO_2) 0.11	[45]
K-/Na-/Ca-/Mg-/clinoptilolite	**Green alkali modification** • Mechanical activation • Alkali modification (nitrate salts of Ca, Mg, K, and Na) under ultrasonic irradiation and magnetic stirring (500 rpm) for 1 h • Green-tea solution reducing agent for 4 h with mixing, ageing for 24 h • Extensive washing, and drying (70 °C for 12 h)	Mg/clinoptilolite Content (EDX), %: (Mg) 8.7, (Si) 20.8, (Al) 5.0, (K) 4.3, (Fe) 3.1, (O) 49.4 2θ / ° (XRD): (clinoptilolite) 24, 28.15; (MgO) 29.8, 43.13 Specific surface: 342.5 $m^2 g^{-1}$ Total volume: 0.05 $cm^3 g^{-1}$ Average pore size: 19.6 nm Basicity: 4.34 mmol g^{-1} λ (FTIR) / cm^{-1}: (water) 3412, 1640 3412, 1640; (zeolitic structure) 1041, 466	[48]
KOH/zeolite Bandung (Indonesia) natural zeolite, mordenite type.	**Zeolite activation** • Sieved (230 mesh) • 6 M HCl for 4 h with stirring **KOH modification** • 50 % KOH + zeolite under ultrasonic radiation • Dried for 24 h and calcined at 450 °C for 4 h	Content (XRF), %: (Si) 40.7; (K) 38.7; (Fe) 10.2; (Ca) 8; (Ti) 1; (Sr) 0.5 2θ / °(XRD): (KOH) 31, 34, 38; (zeolite) 13.4, 19.6, 22.2, 25, 26.2, 27.6, 30.8	[46]
NaOH/zeolite Natural clinoptilolite from Lampung, Indonesia	**Pretreatment** • Immersed in 1 % HF for 30 min, washed, and dried for 2 h **Impregnation** • 2 M NaOH + zeolite for 24 h and dried for 2 h	Content (XRF), %: (Na) 20.5	[53]
K/zeolite Mordenite type	**Incipient wetness impregnation** • Natural zeolite was sieved (150-200 mesh) • 0.5 M H_2SO_4 activation at 90 °C for 4 h • Washed & dried • Stirring with KNO_3 for 24 h • Calcination at 400 °C for 4 h	Content (AAS), %: (K) 4.76 Specific surface area (BET): 111.6 $m^2 g^{-1}$ Average pore size: 8.3 nm 2θ / ° (XRD): (K_2O) 31, 39, 51, 55; (zeolite) 12.4, 19.4, 29.9, 37.1, 45, 56, 60.6; λ (FTIR) / cm^{-1}: (broad peak) 3400-3700, 1080, 550	[47]
KOH/zeolite Natural zeolite Bayah Banten (Indonesia)	**Impregnation** • Natural zeolite was sieved (<50 mesh) • Dried at 110 °C for 24 h • KOH solution impregnated at 60 °C for 26 h • Vacuum separated, dried for 24 h and calcined at 450 °C for 4 h	-	[49]
K_2O/zeolite	**Impregnation** • Natural zeolite was crushed and dried • KOH solution impregnated at room temp, dried for 24 h and calcined at 500 °C for 3 h	Acid number of WCO: 2.92 mg KOH g^{-1} Crystal phase (XRD): no K_2O or KOH peaks are observed	[50]
K_2CO_3/zeolite Natural zeolite from Tapanuli Utara, North Sumatera, Indonesia	• Zeolite was treated with 30 % (v/v) H_2O_2, separated, dried for 24 h, and milled (140 mesh) **Impregnation** • Treated zeolite + (45 g / 60 ml H_2O) K_2CO_3 (w/w=1:4), mixed at 60 °C for 2 h • Dried at 60 °C for 24 h, vacuum filtrated, dried at 110 °C for 24 h, and calcined at 450 °C for 4 h • Milled (140 mesh)	Content (AAS): 11.24 % K_2CO_3	[51]
Zeolite	**Zeolite activation** • Natural zeolite crushed and dipped with H_2SO_4 for 0.5 h, aged for 24 h • Calcined at 450 °C for 2 h	-	[54]

Catalyst designation and origin	Catalyst preparation	Catalyst characteristics	Ref.
Na-zeolite/Fe$_2$(SO$_4$)$_3$ Natural zeolite from Kenya Clinoptilolite and kaolinite type	**Zeolite activation** • Natural zeolite crushed, sieved (0.25-0.5 mm), washed and dried for 24 h • Acid treated: 16 % HCl at room temp. for 12 h, washed, dried, and calcined at 300 °C for 4 h **Cation exchange** • H-zeolite: 0.1 M NH$_4$NO$_3$ refluxed at 80 °C for 3 h, dried, and calcined at 300°C for 4 h • Na-zeolite: 1 M NaCl refluxed at 90 °C for 72 h, washed, dried for 4 h and calcined at 300°C for 3 h • Fe$_2$(SO$_4$)$_3$ was added into reactor (w/w =1/2)	Natural zeolite: Si/Al = 3.98 Content (ICP-AES), %: (SiO$_2$) 62.2, (Al$_2$O$_3$) 13.3, (CaO) 12.0, (Fe$_2$O$_3$) 4.8, (Na$_2$O) 3.1, (MgO) - 1.6 λ (FTIR) / cm^{-1}: bands typical for zeolites at 3000-4000 (broad band), 1640, 500-1100, 400-500	[55]
Zeolite 2 % Ru/zeolite 2 % Ag/zeolite 2 % Pd/zeolite 2 % Pt/zeolite	**Impregnation** • Precursor salts: hexachloroplatinic acid, ruthenium chloride, palladium nitrate, and silver nitrate • Dried for 2 h, calcined in air at 400 °C for 4 h, and before the reaction reduced in 5 % H$_2$-95 % Ar at 300 °C for 1.5 h	Specific surface area (BET), m^2 g^{-1}: 25.95 (Z), 26.37 (Ru/Z), 21.32 (Ag/Z), 21.35 (Pd/Z), and 16.11 (Pt/Z) Average pore radius, nm: 4.09 (Z), 5.84 (Ru/Z), 6.20 (Ag/Z), 6.38 (Pd/Z), and 6.67 (Pt/Z) NH$_3$-TPD total acidity, mmol g^{-1}: 1.0 (Z), 2.3 (Ru/Z), 1.9 (Ag/Z), 1.9 (Pd/Z), and 2.1 (Pt/Z) CO$_2$-TPD, total basicity, mmol g^{-1}: 0.8 (Z), 0.6 (Ru/Z), 0.5 (Ag/Z), 0.5 (Pd/Z), and 0.6 (Pt/Z) Natural zeolite: XPS: Si/Al = 4.42 Identified crystal phase(XRD): mordenite, calcite, clinoptilolite and quartz	[56]

Table 4. Review of the optimal reaction conditions when using natural zeolitic materials as a catalyst/catalyst support

Catalyst designation	Feedstock	Reactor type	Optimal reaction conditions				Yield (con-version), %	Ref.
			T / °C	CC*, wt.%	$t(\tau)$ / min	Alcohol to oil molar (volume) ratio		
Continuous processes								
KOH/clinoptilolite	WCO metha-nolysis Acid value of 3.12 mg KOH/g	Microreactor	65	8.1	(13.4)	(2.25:1)	(97.4)	[45]
Batch processes								
Mg/clinoptilolite	WCO methanolysis	Stirred batch reactor	70	4	120	16:1	98.7	[48]
70 % KOH/zeolite Mordenite from Bandung, Indinesia	Castor oil methanolysis	Stirred batch reactor	55	17	420	15:1	92.11	[46]
NaOH/zeolite Natural clinoptilolite from Lampung, Indonesia	Microalgal oil (*Chlorella vulgaris*) methanolysis	Stirred batch reactor	60	3	4	(50:1)	36.8	[53]
K/zeolite	Rice bran oil methanolysis	Stirred batch reactor	67.5	5	240	12:1	83.2	[47]
KOH/ zeolite Natural zeolite bayah banten, Indonesia	WCO methanolysis	Stirred batch reactor	60	3	120	7:1	94.8	[49]
K$_2$O/zeolite	WCO methano-lysis (HCl este-rification as a pretreatment	Stirred batch reactor	65	2.5	120	8:1	95	[50]
K$_2$CO$_3$/zeolite Natural zeolite from Tapanuli Utara, North Sumatera	Rice bran oil methanolysis	Batch stirred reactor (500 rpm)	65	4	180	10:1	98.2	[51]
Zeolite	Palm oil methanolysis	Batch stirred reactor (200 rpm)	65	0.75	120	14:1	85	[54]
Na-zeolite/Fe$_2$(SO$_4$)$_3$ Natural zeolite from Kenya	*Jatropha curcas* oil methanolysis	Batch stirred reactor (600 rpm)	65	28.9	330	6:1	57	[55]

Catalyst designation	Feedstock	Reactor type	Optimal reaction conditions				Yield (conversion), %	Ref.
			T / °C	CC*, wt.%	$t(\tau)$ / min	Alcohol to oil molar (volume) ratio		
Zeolite 2 % Ru/zeolite 2 % Ag/zeolite 2 % Pd/zeolite 2 % Pt/zeolite	Rapeseed oil methanolysis	Autoclave	260	-	120	9:1	Zeolite-67.2 Ru/zeolite-71.0 Ag/zeolite-71.6 Pd/zeolite-73.8 Pt/zeolite-94.6	[56]

*Catalyst content

Natural zeolite from Bandung Indonesia modified with KOH was used for castor oil methanolysis [46]. By using demanding castor oil (about 84 % of ricinoleic acid) over the zeolite catalyst loaded with high content of KOH (70 wt.%), the FAME content of 92.1 % was obtained, but at a somewhat longer reaction time of 7 h. Unusual, but a reaction temperature (55 °C) slightly below the boiling point of methanol was shown to provide the best results in this case. Potassium as active species in KNO_3 loaded natural zeolite mordenite type from Indonesia did not show activity as similar catalysts [47]. In the reaction with rice bran oil under mild reaction conditions, but at a slightly higher temperature (67.5 °C), a FAME yield of 83.2 % in 4 h was obtained. On the other side, another potassium-modified natural zeolite catalyst, showed significantly better activity [48]. Also, under mild reaction conditions (catalyst loading of 4 wt.%, methanol to waste cooking oil molar ratio of 16:1, and reaction temperature of 70 °C) the catalyst achieved a biodiesel yield of 93.6 % in 2 h. A similar catalyst in the same study showed even better performance, *i.e.*, magnesium-modified natural zeolite achieved a biodiesel yield of 98.7 % under the same reaction conditions. The authors of this study gave the synthesized materials a green and environmental insignia, because they used a green alkali modification synthesis method based on one step using a green tea-based reducing reagent. In addition, the catalysts showed very good reusability.

Also, good activity results were obtained by another potassium-loaded zeolite catalyst, obtained by impregnation of natural Bayah Banten zeolite from Indonesia by KOH [49]. The FAME yield of 94.8 % was achieved in 2 h of reaction with WCO. A similar short study [50], in terms of the catalytic material and reactor system, showed a great potential of a KOH/natural zeolite catalyst for biodiesel production. In specific, 25 % nominal KOH impregnated on natural zeolite from Indonesia achieved a high biodiesel yield of 95 % in 2 h of reaction with a rather low methanol to oil ratio of 8:1 and catalyst loading of 2.5 wt.%. It should be noted that WCO was pretreated with HCl to esterify FFA. The rice bran oil methanolysis over K_2CO_3 loaded on natural zeolite from North Sumatra, Indonesia, under mild reaction conditions resulted in a biodiesel yield of 98.2 % in 3 h [51]. All these presented studies were conducted in simple batch-stirred reactors, except for one study that was performed under continuous reaction conditions [42]. A KOH/clinoptilolite catalyst (clinoptilolite originating from Semnan, Iran) was used in a microreactor for the methanolysis reaction with WCO [45]. The microreactor consisted of a micromixer and a microtube (5 m long, 0.8 mm in diameter) and was equipped with a peristaltic pump to transport reactants. In this study, the already demonstrated advantage of microreactors as compared to classical batch-stirred reactors were confirmed [52]. This is reflected in the required time to reach the reaction equilibrium of 2 h in a batch-stirred reactor, while it took only 13.4 min in the microreactor in which case a biodiesel yield of 97.4 % was achieved. It should be considered that WCO with an acid value of 3.12 mg KOH g^{-1} was used in the reaction.

Sustainable biodiesel production was investigated in a study combining the use of natural zeolite as a catalyst and microalgal oil (*Nannochloropsis oculate* and *Chlorella vulgaris*) as a feed [53]. Natural clinoptilolite from Lampung in Indonesia was simply activated by NaOH even without the usual thermal activation, which certainly resulted in significant energy savings. In this study, *Chlorella vulgaris* oil showed better potential than *Nannochloropsis oculate* oil as a feedstock resulting in 98 % FAME yield as compared to 83.5 % obtained in the latter case under the same mild reaction conditions with a rather higher lipid to methanol volume ratio of 1:50.

A neat simply acid-activated natural zeolite exhibited, surprisingly, solid performance in the reaction with palm oil and methanol [54]. Under mild reaction conditions and 2 h of reaction time, the FAME yield was 82.5 %.

A catalyst obtained in a relatively complex manner (Table 4), based on cation exchange with Na in natural clinoptilolite from Kenya followed by additional chemical modification with $Fe_2(SO_4)_3$, was used in difficult reaction conditions with very high FFAs level (about 14 %) in Jatropha oil [55]. It was shown that such a demanding oil for the transesterification reaction with the proposed catalyst should have been pretreated by esterification. The highest FAME

yield of only 57 % was achieved in 6 h of reaction, and, based on the FAME profile *vs.* time, the reaction has reached equilibrium. It turned out that the added $Fe_2(SO_4)_3$ in a w/w ratio of 1:2 was unable to catalyse esterification and the overall catalytic activity was primarily in the transesterification reaction.

Noble metals, like Pd, Ru, and Ag, supported by natural zeolite exhibited modest activity in the methanolysis of vegetable oil, bearing in mind that the reaction took place in an autoclave at an elevated temperature (260 °C) and only Pt/zeolite was achieved the FAME yield of 94.6 % in 2 h [56]. Interestingly, the neat natural zeolite achieving a FAME yield of 67.2 % was even more active than the Pd/zeolite catalyst, and it was approximately as active as the other two investigated catalysts, Ru/zeolite and Ag/zeolite. These catalysts exhibited an unusual reaction behaviour in their selectivity, inducing a TG conversion higher than 95.3 %.

3. 2. Synthetic zeolite-based catalysts

Synthetic zeolitic-based materials are a very important group, especially as they have been widely exploited in many large-scale industrial processes [25,57]. Many zeolite framework types exist, but for catalytic purposes currently commercially are employed only a dozen such as Beta, ZSM, FAU, MFI, MOR, *etc.* [25]. The average pore diameter in these zeolites is about 1.0 nm (Table 5), which can be a problem for applications in reactions involving large molecules. TG and FAME molecules are relatively large [58], so preparation or use of mesostructured materials is a necessity in these cases to overcome diffusion limitations. Generally, synthetic zeolite-based catalysts showed very high activity, reaching the reaction equilibrium in only 30 min, but in some cases, the biodiesel yield was insignificant, which largely depended on the reaction conditions, the used reactor system, and the type of oily feedstock (Table 6). These catalysts exhibited a very high specific surface area (Table 5) compared to the other zeolite-based catalysts (Tables 3, 7, and 8) and, correspondingly, a smaller pore diameter. Interestingly, such morphological characteristics did not negatively affect the catalyst activity, because the small pore diameter limiting the access of molecules from the reaction mixture was compensated by the large external surface area of the catalyst, which was one to two orders of magnitude greater than that of, for example, natural zeolite-based catalysts.

Biodiesel production from low-quality fatty substrates, such as waste oils or some inedible oils, is certainly challenging. A relatively new approach was proposed and termed hydro-esterification involving hydrolysis of TG in the first step, and esterification of FFA in the second [59]. The hydrolysis step is insensitive to the moisture content or low pH of the feedstock, so impurities are removed from the oily feed in a robust process.

Table 5. Review of preparation routes and characteristics of synthetic zeolite-based catalysts

Catalyst designation and origin	Catalyst preparation	Catalyst characteristics	Ref.
H-ZSM-5 SiO_2 to Al_2O_3 ratio (SAR) of 15 SAR of 140	Commercial catalyst • Calcined in the air at 550 °C for 5 h with a heating rate of 2 °C min^{-1}	Structural parameters: Surface area, $m^2\,g^{-1}$: (SAR 15) 410; (SAR 140) 450 Micropore volume, $cm^3\,g^{-1}$: (SAR 15) 0.09; (SAR 140) 0.12 Pore size, nm: (SAR 15) 0.51×0.55; (SAR 140) 0.53×0.56 NH3-TPD, mmol g^{-1}: (SAR 15) Brønsted sites 0.27; (SAR 140) Brønsted sites 0.99	[59]
Gismondine-based: Na-MAP K-MAP CsK-MAP K-A CsK-A FAU-based: Na-X K-X CsNa-X Na-Y K-Y CsNa-Y	Cs- and CsK-containing zeolites: • Na-form of zeolites A, MAP, X, and Y was treated with the solutions of $CsNo_3$ and CsOH (4/1 v/v) at 80 °C for 1 h. • Washed and dried overnight at 80 °C. • Calcination in the air at 450 °C for 2 h with a heating rate of 1 °C min^{-1}. Other zeolites were commercial	TGA: (Na-MAP) ≈20 wt.% H_2O loss (25-350 °C) Content (EDX), Si/Al: (Na-MAP) 1.0; (K-MAP) 1.0; (CsK-MAP) 1.0; (K-A) 1.0; (CsK-A) 1.0; (K-Y) 2.5; (CsNa-Y) 2.5; (K-X) 1.2; (CsNa-X) 1.2 Na/Al: (Na-MAP) 1.0; (K-MAP, CsK-MAP) 0.1; (K-A) 0.55; (CsK-A) 0.5; (K-Y) 0.2; (CsNa-Y) 0.35; (K-X) 0.4; (CsNa-X) 0.6 N_2-physisorption, BET, $m^2\,g^{-1}$: (K-A) 15; (K-MAP) 45; (K-X) 615, (K-Y) 670. Total basicity (TPD-CO_2), µmol g^{-1}: (Na-MAP) 235, (Na-X) 275; (Na-Y) 320; (K-Y) 345; (K-X) 390; (K-A) 420, (K-MAP) 430	[62]

Catalyst designation and origin	Catalyst preparation	Catalyst characteristics	Ref.
Mo-NaBeta	**NaBeta zeolite support** • NaOH + NaAlO$_2$ + tetraethylammonium hydroxide (TPAOH) stirred at room temp. for 1 h. • Silica gel is added, stirred (1 h). • A cationic copolymer containing quaternary ammonium groups (RCC) added dropwise [the resulting gel - Al$_2$O$_3$/32SiO$_2$/2Na$_2$O/0.01RCC/2.6TPAOH/296H$_2$O] • Autoclave crystallization at 140 °C for 6 days. • Filtered, dried, and calcined at 550 °C for 6 h. **Mo-NaBeta catalyst** • Incipient wetness impregnation method with ammonium molybdate. • Aged for 24 h, dried, and calcined at 550 °C for 3 h.	2θ / ° (XRD): (NaBeta zeolite) 7.7, 21.4, 22.5, 25.4, 27.1 λ (Raman) / cm^{-1}: (MoO$_3$ phase) 116, 129, 157, 246, 278, 338, 381, 668, 821, 997 Specific surface area (BET): 453 m^2 g^{-1} Average pore diameter: 5.4 nm $V_{mesopore}$: 0.18 cm^3 g^{-1} $V_{micropore}$: 0.13 cm^3 g^{-1} H4 hysteresis	[63]
HPW/ZIF-67 (HPW modified Co-based zeolite imidazole framework)	**ZIF-67 synthesis** • Cobalt nitrate + methanol and 2-methylimidazole + methanol were ultrasound treated for 15 min. • Stirred at ambient temp. for 4 h, centrifuged, washed x3, and dried overnight at 130 °C. **HPW/ZIF-67 synthesis** • HPW + ZIF-67 was ultrasound treated for 30 min. • Stirred at ambient temp. for 24 h, centrifuged, washed x3, dried in vacuum at 200 °C.	Specific surface area (BET): 1137 m^2 g^{-1} (88.7 % micropore) Average pore size: 3.16 nm Ishoterm Type I with H3 hysteresis Basicity: 2.46 mmol g^{-1} (Lewis/Brønsted acid ratio=0.18) λ (FTIR) / cm^{-1}: (HPW) 808, 889, 947, 1043	[67]
CaO/zeolite (ZSM-5; CAS No. 1318-02-1)	• Zeolite activation by calcination in air at 500 °C for 4 h (autoclave). **Impregnation** • Calcium acetate + zeolite solution was aged for 12 h. • Dried and calcined in the air at 700 °C for 3 h.	35 % CaO/zeolite λ (FTIR) / cm^{-1}: (bi-carbonate group) 1640 and 1400; (Ca-O group) 528 TPD-CO$_2$: (Desorption peaks) 87, 336, 634, 695 and 886 °C	[61]
HMCM-36 (MWW zeolite type)	**MCM-22(P)** • Hydrothermal synthesis NaAlO$_2$ + H$_2$O and NaOH + H$_2$O mixed, hexamethylenimine added and stirred for 45 min, Aerosil 200 + H$_2$O was added under vigorous stirring for 2 h. Resulting gel (1 SiO$_2$/0.09 Na$_2$O/0.5 HMI/45 H$_2$O/0.01 Al$_2$O$_3$) Crystallization: stirred (600 rpm) at 135 °C for 8 days, washed, and dried overnight at 75 °C. **MCM-36** • Swelling: MCM-22(P) + CTAB + TPAOH + H$_2$O (w/w; 1/5.61/2.44/21.4) stirred at 40 °C for 48 h; washed and dried at 75 °C. • Pillaring: swollen material + TEOS was stirred at 80 °C for 24 h; filtered, dried at 30 °C for 12 h. Samples + H$_2$O (w/w; 1/10) hydrolysed at 40 °C for 5 h, and dried at 30 °C. • Two-step calcinations: 6 h at 450 °C in N$_2$ (1 °C min^{-1}) and 12 h at 550 °C in the air (2 °C min^{-1}). **HMCM-36** • Ion exchange: 1 M NH$_4$NO$_3$ solution for 8 h (pH 7, NH$_4$OH), filtered, dried and calcined at 500 °C for 5 h	Specific surface area (BET), m^2 g^{-1}: 635, 205 (micropore), 430 (mesopore) Isotherm Type IV DRIFT pyridine ads., µmol g^{-1}: (Brønsted sites) 34.3; (Lewis sites) 10.2 λ (FTIR) / cm^{-1}: 1087, 805, 595, 554	[65]
Lipozyme-TL/FM-8 (Commercial FM-8 zeolite, mordenite type)	**Lipase immobilization** • Zeolite + lipase enzyme (2.5 mg mL^{-1}) + 0.1 M phosphate buffer (pH 7) aged for 18 h at room temp	Chemical composition of zeolite: Na$_{0.17}$[(AlO$_2$)$_{1.10}$(SiO$_2$)$_{0.45}$]1.34H$_2$O	[66]
Ba-Sr/ZSM-5	**Incipient wetness impregnation method** • ZSM-5 zeolite calcined at 600 °C for 6 h • Impregnated with 6 wt.% of Sr(NO$_3$)$_2$ • Impregnated with 4 wt.% of Ba(NO$_3$)$_2$ • dried for 12 h and calcined at 600 °C for 6 h	Specific surface area (BET): 224.2 m^2 g^{-1} Average pore diameter: 1.89 nm Phase (XRD): identified phase - Al$_2$SiO$_8$, BaO, SrO (monoclinic), and Al$_2$O$_3$SiO$_2$ (orthorhombic) λ (FTIR) / cm^{-1}: (H$_2$O) broad band at 3454 & 1636, (Lewis acid sites) ≈1490, (Brønsted acid sites) 1540-1630, (SrO & BaO) 520-600	[60]

Catalyst designation and origin	Catalyst preparation	Catalyst characteristics	Ref.
2D Na/ITQ-2 (Two-dimensional MWW-type structure)	**Rotational hydrothermal synthesis of 2D zeolite** • Hexamethyleneimine (HMI) as an organic structure-direction agent, starting gel was 1.0 Al_2O_3 : 30 SiO_2 : 2.5 Na_2O : 10 HMI : 580 H_2O • NaOH & $NaAlO_2$ were dissolved in H_2O + colloidal silica (40 wt.%) & HMI and stirred for 3 h • Crystallization: stirred autoclave at 140 °C for 4 days • Centrifuged, washed with H_2O & ethanol and dried at 80 °C • A precursor was suspended in aqueous cetyltrimethylammonium hydroxide/tetrapropylammonium hydroxide at 85 °C for 16 h • Delamination: ultrasound bath for 1 h at 50 °C & pH of 12.5 • Washed, dried and calcined at 600 °C for 8 h **Solid-state ion exchange** • Ion exchange with 1 M NH_4NO_3 at 80 °C for 8 h • 1 mmol alkali & alkaline-earth acetate was mixed with zeolite support and grinded (1:1 of molar ratio) • Calcined at 600 °C for 10 h	Content (ICP-OES), 2.1 wt.%: Na, Na/Al = 1.2, Si/Al = 22 Specific surface area (BET): 613 $m^2\ g^{-1}$ V_{meso} / $cm^3\ g^{-1}$: 0.77 V_{micro} / $cm^3\ g^{-1}$: 0.08 Type IV isotherm	[64]

Table 6. Review of optimal reaction conditions when using synthetic zeolite-based materials as catalysts/catalyst supports

Catalyst designation	Feedstock	Reactor type	Optimal reaction conditions				Yield (conversion), %	Ref.
			T / °C	CC*, wt.%	t / min	Alcohol to oil molar ratio		
H-ZSM-5	WCO methanolysis	Stirred batch • Two-step reaction • Hydrolysis (H) with water • Esterification I with ethanol	H-100 E-77	H & E=5	240	H (water to oil)-3:1 E-3:1	H-(40) E-(63)	[59]
K-MAP (K-form of synthetic gismondine based on the maximum Al P)	Refined rapeseed oil methanolysis	Pressured stirred batch high power density (Biotege Initiator + single-mode microwave system)	160	5	15	12:1	(96), [TOF, h^{-1} = 202]	[62]
7 % Mo-NaBeta	Rice bran oil methanolysis	Stirred autoclave (300 rpm)	140	1.5	480	13.7:1	(84.6)	[63]
0.25 HPW/ZIF-67	Microalgal oil (*Chlorella vulgaris*) esterification and methanolysis	Autoclave	200	1	90	20:1	(98.5)	[67]
CaO/zeolite	Waste lard methanolysis	Microwave (595 W)	-	8	75	30:1	90.1	[61]
HMCM-36	Palmitic acid esterification	Stirred batch reactor	80		360	30:1	(100)	[65]
Lipozyme-TL/FM-8	WCO methanolysis	Stirred batch (200 rpm)	Room (24)	4	1440	4:1	Insignificant (≈0.65)	[66]
Ba-Sr/ZSM-5 (6 wt.% Sr; 4 wt.% Ba)	Sunflower oil methanolysis	Stirred batch (500 rpm)	60	3	180	9:1	87.7	[60]
2D Na/ITQ-2 (2D MWW-type structure)	Triolein methanolysis	Stirred batch (1000 rpm)	60	15	60	10:1	95	[64]

*Catalyst content

In that manner, this step circumvents soap formation as a major drawback of common and commercialised biodiesel production processes. A commercial H-ZSM-5 catalyst was used for the hydro-esterification of WCO under relatively mild reaction conditions (under 100 °C). Structurally the catalyst had a small pore size (about 0.55 nm) unfavourable for this kind of reaction, and consequently very high surface area, but the displayed activity was surprising. In 4 h of reactions, WCO hydrolysis with 40 % conversion into a fatty acid mixture and 63 % conversion of the synthesized fatty acids in esterification to biodiesel was observed. ZSM-5 zeolite supporting Ba and Sr was used in another study [60] showing solid activity under mild reaction conditions.

Yet, more interesting, the biodiesel yield did not fluctuate much with the change in reaction parameters such as the methanol to oil molar ratio, reaction time, and even the reaction temperature. The highest biodiesel yield (87.7 %) was achieved in 3 h of reaction. The best methanol to oil molar ratio was found to be 9:1, but in the whole interval from 3:1 to 21:1 ratio, the yield was almost constant, even at the theoretical molar ratio of 3:1. Also, the influence of reaction

temperature in the range from 50 °C to 65 °C was negligible. ZSM-5 zeolite impregnated with CaO showed a biodiesel yield of 97.1 % from waste lard under mild reaction conditions in 1.25 h of reaction in a microwave reactor [61]. To achieve such a good activity of the catalyst in a relatively short reaction time, it was necessary to load 35 wt.% CaO on the zeolite surface.

Table 7. Review of preparation routes and characteristics of zeolitic materials obtained from natural or waste sources

Catalyst designation and origin	Catalyst preparation	Catalyst characteristics	Ref.
Co-Ni-Pt-FAU FAU-type zeolite prepared from shale rock (Wexford, Ireland)	**Zeolite** • Shale was crushed, sieved (<90 μm), and calcined in air at 800 °C for 4 h • Deferrization: 5 M HCl at 85 °C for 4 h • Alkali activation: 1:1.5 m/m, 40 wt.% NaOH, heated in air at 850 °C for 3 h, crushed • Fused shale + sodium silicate + water, stirred (3 h), aged at room temp. for 18 h • Hydrothermal treatment: 100 °C for 24 h **NH$_4^+$ zeolite (H-FAU)** • 3x (2 M ammonium chloride+ zeolite stirred at room temp. for 2 h, washed) • Washed, dried, and calcined in air at 500 °C for 4 h **Co-Ni-Pt-FAU** • Incipient wetness method (Co, Ni, and Pt precursors in 0.1 M HCl), loadings of 1 wt.% • Dried and calcined in air at 500 °C for 4 h	Specific surface area (BET), m^{2}g^{-1}: (H-FAU) 571; (CO-Ni-Pt-FAU) 490	[57]
Zeolite Steel furnace slag	• Furnace slag was ground (<90 μm) and calcined at 700 °C for 3 h • 3 M HCl at 100 °C for 2 h • Hydrated silica-gel (90 % of silica) was separated, filtered, rinsed 2×, dried, powdered and dissolved in 6 M NaOH + NaAlO$_2$ • The solution was stirred at room temp. for 1 h and another 1 h at 90 °C **Crystallization** • In autoclave at 100 °C for 6 h, filtered, washed, dried, and calcined at 450 °C for 4 h	$2\theta/$ ° (XRD): (zeolite structure) 24.7, 29.6, 39.2, 57.1 Mass loss temperature (TGA), °C: 100-150, 450, and 800 Specific surface area (BET): 10.3 m^{2}g^{-1}	[72]
HY-kaolin Zeolite prepared from Iraqi kaolin clay, faujasite structure	**NaY zeolite** • Sieved kaolin + 40 wt.% NaOH (w/w=1:1.5) was heated at 850 °C for 3 h; milled • Activated kaolin + Na silicate + H$_2$O was stirred at 50 °C for 1 h (pH=13.3); aged at 50 °C for 24 h and crystallized at 100 °C for 48 h • Washed, dried at 110 °C for 16 h, and calcined in air at 500 °C for 1 h **HY zeolite** • NaY + 1 M NH$_4$NO$_3$ was stirred at 100 °C for 4 h • NH$_4$Y zeolite was washed, dried at 100 °C for 6 h, and stirred with 0.5 N oxalic acid at room temp. for 8 h • Washed, dried, and calcined in air at 550 °C for 5 h	Content (XRF), %: (Al$_2$O$_3$) 15.92; (SiO$_2$) 58.11; (CaO) 4.11; (Fe$_2$O$_3$) 3.19, (MgO) 1.22 $2\theta/$ ° (XRD): 6.3, 15.8, 23.8 Specific surface area (BET): 390 m^{2}g^{-1}65 % of zeolite Y purity	[74]
Zeolite/chitosan/KOH Clinoptilolite zeolite	**Impregnation** • Zeolite/chitosan powder + KOH aqueous solution (w/w=1:4) was stirred at 60 °C for 24 h; dried and calcined at 450 °C for 4 h	$2\theta/$ ° (XRD): (chitosan) 10, 20; (zeolite) 6.6, 9.8, 22.2, 22.4, 25.7, 26.6, 27.6, 28.1, 29.9; (K$_2$O) 31.5, 32.4 λ (FTIR) / cm^{-1}: 2874, 1668, 1348, 1021, 821, 703, 460.8	[68]
LTA-kaolin Linde type A zeolite from kaolin	• Kaolin calcination at for 800 °C for 10 h **Hydrothermal synthesis** • 1.4 wt.% kaolin + H$_2$O + NaOH (kaolin/NaOH=1/2) at 90 °C for 24 h; washed and dried at 110 °C for 24 h • Calcination at 400 °C for 6 h	Specific surface area (BET): 44.9 m^{2}g^{-1} Content (NMR): Si/Al = 1.16 λ (FTIR) / cm^{-1}: 1076, 804, 557, 474	[73]
Na/zeolite-chitosan Clinoptilolite zeolite	**Impregnation** • Chitosan + zeolite + methanol (5 % v/v) mixed for 3 h + methanol (5 %) mixed for another 2 h • 0.5 M NaOH added drop-wise, mixed (100 rpm) for 3 h, dried at room temp.	Content (EDX), wt.%: I 37.2, (Na) 11.7, (Si) 10.3, (Al) 1.9, (O) 37.5 Mass loss (TGA): 5 % at 700 °C Specific surface area (BET): 3.73 m^{2}g^{-1} (8.3 for zeolite) λ (FTIR) / cm^{-1}: 1560, 1021, 643	[69]

Catalyst designation and origin	Catalyst preparation	Catalyst characteristics	Ref.
Na/CAN Cancrinite-type zeolite Natural diatomaceous earth (Vietnam)	**Hydrothermal synthesis** • Sieved with mesh No. 50 • Diatomite + NaOH + Al_2O_3 + H_2O stirred at 800 rpm for 30 min at room temp. and aged for 30 min • Hydrothermal reaction at 220 °C for 12 h • Washed, dried and calcined at 500 °C for 6 h	Phase (XRD): the complete transformation of diatomite to CAN zeolite λ (FTIR) / cm^{-1}: Typical CAN zeolite bands at 1036, 1003 and 966, 760, 683 TGA: evaporation of H_2O bounded in pores at 300-400 °C; dehydroxylation of silanol groups at ≈575 °C and change in aluminium structure on zeolite) at ≈800 °C Specific surface area (BET), $m^2 g^{-1}$: 29.83 (fresh), 30.41 (spent)	[77]
FAU-type zeolite Irish shale rock	**Hydrothermal synthesis** • Clean shale was crushed, sieved (<90 µm) and calcined in air at 800 °C for 4 h • Acid treated: 5 M HCl at 85 °C for 4 h • Alkali fusion: 40 wt.% NaOH (1/1.5 w/w), heated at 850 °C for 3 h, crushed • Hydrothermal treatment: fused shale + Na_2SiO_3 + H_2O stirred at room temp. for 3 h, aged for 18 h, hydrothermally treated at 100 °C for 24 h **NH_4 form** • Prepared zeolite + 2 M NH_4Cl stirred at room temp. for 2 h, the procedure was repeated 3 times • Washed, dried, and calcined at 500 °C for 4 h	Si/Al = 1.98 Specific surface area (BET): 571 $m^2 g^{-1}$ Average particle size: 2 µm	[76]
Ni/zeolite Geothermal solid waste	**Hydrothermal synthesis** • Si/Al molar ratio of 10:1 • Solution of NaOH (heated at 100 °C and stirred at 300 rpm) + $Al(OH)_3$ + geothermal waste was stirred for 2 h at 30 °C • Hydrothermal process: autoclave at 100 °C for 6 h • Washed until pH=7 and calcined at 500 °C for 5 h **Impregnation** • $Ni(NO_3)_2$ solution (5 % w/w) at 60 °C for 4 h • Calcined at 500 °C for 5 h	Geothermal solid waste composition, %: (SiO_2) 75.1; I 23.3; (Na_2O) 0.3; (Cl) 0.2; (Al_2O_3) 0.1 2θ / ° (XRD): (analcime) 15.9, 26.1, 30.1; (NiO) 43.0, 63.0, 75.0, 79.0 EDX: Ni was highly dispersed on the surface Specific surface area (BET): 81.9 $m^2 g^{-1}$ Pore radius: 1.56 nm	[70]
Zeolite Geothermal solid waste (Indonesia)	• Geothermal solid waste was washed, dried, and sieved (40 mesh) **Hydrothermal synthesis** • 3 M NaOH + geothermal waste + $Al(OH)_3$ was mixed (300 rpm) at 100 °C for 2 h • Crystallization in an autoclave at 150 °C for 8 h • Washed (until pH 7-8), dried, and calcined at 550 °C for 5 h	Content (XRF), %: (Fe) 9.3, (K) 8.2, (Cl) 6.7, (Ca) 6.7, (Si) 5.3, (S) 4.9, (P) 3.8, (As) 3.1, (Al) 2.2, (Sb) 2.0, (Zn) 1.9, (Cu) 1.5 Si/Al = 2.39 2θ / ° (XRD): (analcime) 16, 26.1, 30.7 Specific surface area (BET): 224.5 $m^2 g^{-1}$	[71]

Nano-crystalline synthetic gismondine-type MAP zeolite modified *via* cation exchange has been utilised as a highly active and selective catalyst to produce biofuel [62]. K-form of gismondine, based on the maximum aluminium MAP zeolite, exhibited a significant improvement in catalytic performance in the methanolysis of rapeseed oil in comparison with low silica zeolites FAU and LTA. Such behaviour was explained by its nanoparticle morphology and high basicity associated with the high Al content and a high degree of ion exchange. The highest yield of biodiesel (98 %) was obtained in only 30 min, but under microwave irradiation and elevated pressure and temperature of 1,5 MPa (15 bar) and 160 °C, respectively. It should be noted that also a high FAME yield (>95 %) was obtained even after only 15 min of reaction.

NaBeta zeolite was synthesized using a surfactant tetraethylammonium hydroxide in an energetically demanding process since the crystallization lasted for 6 days at 140 °C [63]. Finally, the catalyst was synthesized by impregnation of the zeolite support with molybdenum. The synthesized NaBeta zeolite possessed a very high specific surface area of 650 $m^2 g^{-1}$, while by loading Mo, that surface area was certainly reduced, but it remained significant, higher than 400 $m^2 g^{-1}$. The Mo content was optimized indicating the 7 % Mo/NaBeta zeolite catalyst as the most active, but still, its performance was limited yielding the TG conversion of 84.6 % in 8 h of reaction with rice bran oil in the autoclave at the elevated temperature of 140 °C. At a higher temperature a slightly higher conversion was achieved, however, the attempt to lower the temperature to 110 °C resulted in a very low catalytic activity (the TG conversion of about 37 % in 8 h). Optimisation of several parameters were performed in this study showing that smaller catalyst particles (0.15 to

0.55 mm) exhibited uniform and better activity than 0.65 mm and 0.75 mm particles. Agitation (50-500 rpm) of the reaction mixture in the autoclave did not contribute to increasing the catalyst activity, while higher methanol concentrations contributed to better TG conversion, especially to higher reaction rates in the initial stage.

Table 8. Review of preparation routes and characteristics of fly ash-based zeolitic materials

Catalyst designation and origin	Catalyst preparation	Catalyst characteristics	Ref.
Zeolite • Coal fly ash zeolite, sodalite type	**Hydrothermal process** • Alkali treatment: $NaOH + H_2O + NaAlO_2$ solution and $NaOH + H_2O$ + fly ash solution formed sticky gel structure • Aged for 6 days • Crystallized at 100 °C for 24 h • Washed until pH 9.0 and dried for 24 h	Catalyst 2θ / ° (XRD): (sodalite zeolite) 14.1, 24.5, 31.8, 37.9, 43.2 Specific surface area (BET): 9.7 $m^2 g^{-1}$ Isotherm type-IV Coal fly ash Content (XRF), %: (SiO_2) 68.4, (Al_2O_3) 14.8, (Fe_2O_3) 7.9, (CaO) 3.8, (K_2O) 2.5, (TiO_2) 1.2, (SO_3) 0.6, (MgO) 0.3, (ZrO_2) 0.1 Specific surface area (BET):3.4 $m^2 g^{-1}$	[79]
FA/K-X • Zeolite from South African class F fly ash	**FA/Na-X** • The conventional hydrothermal synthesis procedure **FA/K-X** • FA/Na-X was dried for 2 h + 1 M solution of K acetate (v/v=1/10), aged for 24 h at 70 °C. • Washed, dried at 120 °C for 2 h, and calcined in air at 500 °C for 2 h.	Fly ash SiO_2/Al_2O_3 = 1.65 Specific surface area (BET):257 $m^2 g^{-1}$: Phase (XRD), 2θ°: 12, 14, 24 λ (FTIR) / cm^{-1}: 300-430, 500-600, 620, 740, 950 Base strength: 15.0<$H\_$<18.4	[86]
Li/NaY • Zeolite from Chinese coal fly ash	**Alkali activation:** • Sieved fly ash + 0.5 M NaOH stirred at 80 °C for 1 h; washed and dried at 100 °C for 3 h. • Grounded with NaOH and calcined at 850 °C for 2h. **Hydrothermal synthesis:** • Molar ratio of $Al_2O_3:SiO_2:Na_2O:H_2O$ = 1:8.8:4.3:250; stirring and ageing for 12 h. • Crystallization at 100 °C for 10 h, washed and dried. **Microemulsion-assisted co-precipitation:** • Ultrasound treated for 0.5 h (H_2O + isooctane + polyethylene glycol + *n*-propanol + NaY zeolite + Li_2CO4) • 1 M Na_2CO_3 was added in droplets under stirring at 60 °C for 1 h; aged for 12 h at 60 °C. • Washed x3, vacuum dried for 12 h, and calcined at 750 °C for 4 h (3 °C min^{-1})	Li/NaY molar ratio = 1.1 (TG): major weight loss ≈650 °C and ≈775 °C Phase (XRD): NaY and Li_2CO_3 peaks are not visible, new peaks of $LiAlO_2$, Li_4SiO_4, Li_2SiO_3, and Li_3NaSiO_4 emerged Specific surface area (BET): 105.7 m^2g^{-1} Average Pore size: 6.3 nm Basicity: 12.4 mmol g^{-1}; Basic strength: 15<$H\_$<18.4 λ (FTIR) / cm^{-1}: 3574, 3426, 1446, 952, 628, 512 Fresh and catalyst exposed to air for 10 days had very similar FTIR profile	[85]
CaO/ZM$_{FA}$ • Lignite coal fly ash (Serbia) • CaO from eggshell	**Thermo-chemical treatment** • Fly ash was calcined at 850 °C for 2 h • Acidification: 6 M HCl (S/L=1:5) at 80 °C for 6 h, filtrated, washed (pH neutral), and dried **Alkali activation** • 6 M NaOH (S/L=1:5) at 260 °C for 4 h in the rotating miniature autoclave, filtrated, washed (pH 9), and dried **Ultrasound-assisted impregnation** • Raw eggshells, dried, grounded, and calcined at 900 °C for 4 h • Calcined eggshells + 10 wt.% zeolite alcoholic suspension ultrasonically dispersed for 15 min • Dried and calcined at 550 °C for 4 h	2θ / ° (XRD): (lime) 37.5, 43.7, 63.4 Zeolite crystallite size: 47.8 nm; crystallinity degree of 81 % Catalyst crystallite size: 23.4 nm; crystallinity degree of 83 % λ (FTIR) / cm^{-1}: (Zeolitic structure) 961, 684, 626, 557; (CaO) 1436 Porosity, %: (zeolite) 13.3; (catalyst) 86.5 Specific surface area, $m^2 g^{-1}$: (zeolite) 15.7; (catalyst) 22.6 Av. pore diameter, nm: (zeolite) 13.5; (catalyst) 18.2 H2 hysteresis type; TPD-CO_2, μmol g^{-1}: 62.0	[29]
SC-Na • Zeolite from Korean coal fly ash	• Fly ash + (3 M HCl + 4 M H_2SO_4) (w/w=1/2) mixed at 60 °C for 1.5 h; washed and dried • Precursor + NaOH mixed (w/w=1:3) and calcined at 700 °C for 3 h	Content (XRF), %: (Na_2O) 60.2; (SiO_2) 27.4; (Al_2O_3) 3.6; (Fe_2O_3) 1.4; (TiO_2) 1.4; (CaO) 1.3	[84]
Zeolite X • Indian F-type coal fly ash	**Alkaline fusion:** • Calcined at 850 °C for 2 h • 10 % hydrochloric acid at 80 °C for 1.5 h • Fly ash + NaOH (w/w=1/1.5) at 550 °C for 1 h **Hydrothermal treatment:** • Fusion mixture + H_2O + 20 wt.% Na aluminate was crystallized at 90 °C for 8 h; washed and dried • Calcined at 500 °C for 2 h	Si/Al molar ratio = 3.16 Specific surface area (BET): 727.7 m^2g^{-1} Type II isotherm, H3 hysteresis (XRD): major phase was quartz, crystalline mullite, and less intense hematite and amorphous glassy phase. Average particle diameter: 2-5 μm	[83]

Catalyst designation and origin	Catalyst preparation	Catalyst characteristics	Ref.
AZ-KX • (Acid-treated X zeolite ion-exchanged with K) • Zeolite prepared from Indian coal fly ash	**Zeolite activation** • Calcination at 800 °C for 2 h • Acid treatment: hydrochloric acid (10 %) at 80 °C for 1 h. • Alkaline fusion: fly ash/NaOH=1:1.2; 1 h at 550 °C; 30 wt.% of Na aluminate for Si/Al ratio control • Hydrothermal crystallization: 110 °C for 12 h **Ion exchange** • 1 M Potassium acetate + zeolite (S/L=1:10) heated at 60 °C for 24 h; washed, dried, and calcined at 500 °C for 2 h	Cation exchange capacity: 380.6 meq 100 g^{-1} Specific surface area (BET): 334.7 m^2 g^{-1} Type II isotherm, H3 hysteresis λ (FTIR) / cm^{-1}: 1467, 982, 756, 675 TGA: 9 % at 950 °C	[81]
26Hydroxy sodalite • South African coal fly ash	**Hydrothermal treatment:** • 6 M NaOH + fly ash (1:1.2 w/w) aged (800 rpm, 70 °C, and 1.5 h) • Hydrothermal crystallisation at 140°C for 24 h; washed (until pH 10), and dried	XRD: (crystallinity) 18 %; (crystal size) 21.1 nm Content (EDS), %: (Al) 16.5, (Si) 13.3, (Na) 4.9, (Ca) 2.7, (Fe) 1.1, (Mg) 1.0, (O) 59.4 Si/Al = 0.81	[82]
CaO/FA-ZM • Lignite coal fly ash (Serbia) • CaO from eggshell	**Thermo-chemical treatment** • Fly ash was calcined at 850 °C for 2 h • Acidification: 6 M HCl (S/L=1:5) at 80 °C for 6 h, filtrated, washed (pH neutral), and dried **Alkali activation** • 6 M NaOH (S/L=1:5) at 260 °C for 4 h in the rotating miniature autoclave, filtrated, washed (pH 9), and dried **Hydration-dehydration method** • Raw eggshell was washed, dried, ground, and calcined at 900 °C for 2 h • Hydration: activated eggshells + 10 wt.% zeolite water suspension stirred (700 rpm) at 60 °C for 6 h • Dried and calcined at 650 °C for 4 h	Fly ash was class F Si/Al (zeolite) = 2.28; Si/Al (catalyst) = 1.94 Content (ED XRF), %: (CaO) 50.0, (SiO$_2$) 24.1, (Al$_2$O$_3$) 12.7, (Na$_2$O) 10.1, (Fe$_2$O$_3$) 1.9, (MgO) 1.2 (XRD): lime, gismondine, and ά-dicalcium silicate phases identified λ (FTIR) / cm^{-1}: (Zeolitic structure) 543; (CaO) 1415, 871 Porosity: (zeolite) 82.9 % (catalyst) 87.8 Specific surface area, m^2 g^{-1}: (zeolite) 21.1, (catalyst) 18.7 Average particle size, μm: (zeolite) 36.4, (catalyst) 17.7 Basicity, mmol g^{-1}: (zeolite) 0.36, (catalyst) 23.2	[42]
Kaliophilite • Circulating fluidized bed fly ash (Inner Mongolia, China)	**Fly ash-based geopolymer** • Water glass + KOH (S/L=1.5) + fly ash stirred for 5 min, aged at 80 °C for 24 h **Hydrothermal synthesis** • Geopolymer + 6 M KOH at 180 °C for 24 h, washed, dried, and granulated (0.15-0.315 mm)	2θ / ° (XRD): (kaliophilite) 20.85, 26.5, 26.7, 33.3, 40.9 λ (FTIR) / cm^{-1}: (Kaliophilite structure) 985, 698, 607, 561, 480 (Adsorbed water) 3446, 1656 Specific surface area (BET): 3.5 m^2 g^{-1} Average pore size: 20.9 nm Type IV isotherm, H3 hysteresis Basic strength: 9.8<$H\_$<15	[87]

Zeolites, conventionally used in three-dimensional forms generally induced mass transfer limitations, which affects the overall catalytic activity. To overcome this deficiency, a two-dimensional structure was designed with a large external surface area and hierarchical characteristics [64]. In the study, the solid-state ion-exchange method was adopted for Li$^+$, Na$^+$, K$^+$, Ca^{2+}, and Mg^{2+} loading on zeolite with an MWW-type structure. The investigation of the influence of cation type on the catalyst performance showed the following order in activity: Na$^+$ > K$^+$ > Ca^{2+} >Li$^+$ ≈ Mg^{2+}. The influence of the zeolite carrier type on the activity was also investigated indicating the two-dimensional Na/MWW zeolite catalyst as superior compared to the two-dimensional Na/MCM zeolite catalyst and a three-dimensional Na/Y zeolite catalyst. The most successful two-dimensional Na/MWW catalyst was synthesized by expansion, delamination, and subsequent solid-state ion-exchange approach using hexamethylene imine as an organic structure-directing agent under stirred hydrothermal process. The obtained catalyst possessed a very high total surface area of 613 m^2 g^{-1}, but the most significant result was that the material had the highest percentage of basic sites on the external surface areas. For only 1 h, the two-dimensional Na/MWW zeolite catalyst reached a biodiesel yield of 95 % under mild reaction conditions, in contrast to the three-dimensional Na/Y zeolite catalyst, which achieved a biodiesel yield of only 6 %. Layered MWW zeolite was also used for the esterification of palmitic acid [65]. The zeolite was modified by pillaring and swelling using cetyltrimethylammonium bromide (CTAB) and silica as swelling and pillaring reagents, respectively. In that manner, a mesoporous material was obtained with a very high surface area of 635 m^2 g^{-1} and the increased number of Brønsted and Lewis acid sites, as compared to the other synthesized catalysts (such as MCM zeolite-based catalysts). Under very mild esterification conditions (70 °C and 30:1 methanol to oil molar ratio) the pillared H MWW zeolite

showed high stability in consecutive cycles and 85.3 % conversion of palmitic acid in 6 h of reaction in the first cycle. For a longer reaction time, the total conversion (100 %) was obtained.

The idea to obtain biodiesel enzymatically turned out to be very demanding [66]. Commercial Lipozyme TL containing lipase was immobilized on FM-8 zeolite mordenite-type with Na^+ as a major cation and used for methanolysis of WCO under very mild reaction conditions, which meant room temperature, alcohol to oil molar ratio of 4:1, lipase content of 4 %, 24 h of reaction and mixing at 200 rpm. However, under these reaction conditions, the immobilized lipase on zeolite did not show any activity. It should be also emphasized that the realized immobilization efficiency was unsatisfactory yielding only 56.1 % (95.8 % was obtained for hydrotalcite as support). The very high level of FFA microalgal lipids (*Chlorella vulgaris*, 34 mg KOH g^{-1} and calculated FFA content of 17 %) were successfully converted to biodiesel using a bifunctional phosphotungstic acid-modified zeolite imidazolate framework catalyst [66]. Activity of the bifunctional catalyst was achieved at higher temperatures due to the requirement for activation of catalytically active centres for esterification and transesterification, so that the conversion of 98.5 % is obtained at 200 °C in 1.5 h of reaction. For example, when performing the reaction at the temperature of 80 °C, conversion of only about 10 % was achieved. The best activity was obtained with the optimum phosphotungstic acid (HPW) content in the catalyst of 0.25 wt.% achieving at the same time impressive textural characteristics, with the BET surface area of 1137 m^2 g^{-1} and external surface area of 129 m^2 g^{-1}. Considering the very unfavourable quality of the used microalgal lipids and the demonstrated good stability and recyclability of the material, this catalyst can be considered very promising to produce biodiesel.

3. 3. Zeolite-based catalysts originating from natural and waste sources

Natural zeolites and zeolites derived from waste sources may not have very large specific surface areas and hierarchical structures as synthetic zeolites, but they support sustainable chemistry, contribute to waste reduction solutions, and exhibit suitable characteristics (Table 7) and catalytic activity (Table 9) due to adequate bonding of catalytically active species and the zeolite support. Many studies [68-72] couple natural- or waste-based zeolite catalysts and WCO as feedstock guided by the principles of green chemistry. These catalysts can be applied in qualitatively unfavourable feed oils achieving respectable biodiesel yields in a one-step process (Table 9).

To conduct the process of WCO transesterification under mild reaction conditions, a heterogeneous catalyst was used based on a zeolite/chitosan/KOH composite [68]. The catalyst was synthesized from natural polysaccharide chitosan and natural zeolite clinoptilolite-type with KOH impregnation. FAME was produced at room temperature by an electrolysis process using a graphite electrode, at a relatively low methanol to oil molar ratio (7:1), 2 wt.% of deionised water, and a co-solvent. It has been shown that in 3 h reaction time, with 10 wt.% acetone as a co-solvent and only 1 wt.% of the catalyst, a biodiesel yield of 93 % was achieved. WCO methanolysis was investigated by a geothermal solid waste-derived Ni/zeolite catalyst [67]. The geothermal solid waste from Indonesia contained mainly SiO_2 (75.1 %) and trace amounts of Al_2O_3 and Na_2O. Generally, the high content of Si led to low acidity of zeolite and, consequently, the basicity of the resulting zeolite is increased. The obtained catalyst had a medium-developed surface area (81.9 m^2 g^{-1}) with an average pore radius of about 5 nm. The satisfactory activity of the catalyst was obtained under mild reaction conditions for 4 h of reaction. The study provided a simple cost analysis of the catalyst production comparing it to common commercial catalysts. A comparison of two basic and one acidic homogeneous commercial catalysts indicated that nowadays the production cost of Ni/zeolite catalyst is five times higher than that of NaOH, about 50 % higher than that of H_2SO_4, and 2.2 times lower than that of KOH. However, the situation is somewhat more favourable regarding the biodiesel yield per mass of the catalyst.

The Ni/zeolite catalyst is superior to KOH and H_2SO_4, but NaOH is still more economical. Yet, the presented economic analysis was very limited in scope not considering that homogeneous catalysts need a complex separation process and cannot be reused like heterogeneous catalysts, which consequently raises costs. Thus, a more comprehensive economic analysis should be performed before conclusive statements about the economic efficiency of different catalysts. WCO transesterification was performed in a common stirred batch reactor by using a neat zeolite catalyst obtained from waste steel furnace slag [72]. The composition of the steel furnace slag comprising mainly silica, calcium and aluminium suggested the common procedure for transformation to a zeolite structure: calcination - acid treatment - hydrothermal synthesis - autoclave crystallisation - calcination.

Table 9. Review of reaction conditions when using zeolitic materials obtained from natural or waste sources as catalysts/catalyst supports

Catalyst designation	Feedstock	Reactor type	Optimal reaction conditions					Yield (conversion), %	Ref.
			T / °C	CC*, wt.%	t (τ) / min	Alcohol to oil molar ratio			
Continuous processes									
Co-Ni-Pt-FAU Shere rock originated	Oleic acid ethanolysis	Fix-bed tubular reactor (10×650 mm)	70	-	(180)	-		93	[57]
Batch processes									
Co-Ni-Pt-FAU Shere rock originated	Oleic acid ethanolysis	Batch stirred reactor	70	-	90	6:1		89	[57]
HY-kaoline Fujasite type zeolite from kaolin	Oleic acid esterification (ethanolysis)	Batch stirred reactor	70	5	60	6:1		(85)	[74]
Zeolite/chitosan/KOH Clinoptilolite zeolite	WCO methanolysis (1 wt.% acetone as cosolvent and 2 wt.% of H_2O)	Electrolysis-assisted (40 V, 2 wt.% H_2O) stirred (400 rpm) batch reactor	-	1	180	7:1		93	[68]
LTA-kaolin Linde type A zeolite from kaolin	Triolein methanolysis	Batch stirred reactor (600 rpm)	62.9	72	146	36.6:1		92.8±4.0	[73]
Na/zeolite-chitosan Clinoptilolite zeolite	WCO methanolysis	Electrolysis assisted (40 V, 2 wt.% H_2O + 10 wt.% acetone) stirred batch reactor (400 rpm)	25	1	30	8:1		96.5	[69]
Na/CAN Natural diatomaceous earth (Vietnam) cancrinite-type zeolite	Soybean oil methanolysis	Batch stirred reactor (600 rpm)	63	20	90	20:1		(98)	[77]
FAU-type zeolite Irish shale rock	Oleic acid esterification (ethanol)	Batch stirred reactor	70	5	90	6:1		(78)	[76]
Ni/zeolite Geothermal solid waste	WCO simultaneous methanolysis and esterification	Batch stirred reactor (400 rpm)	60	3	240	12:1		89.4	[70]
Zeolite Geothermal solid waste (Indonesia)	WCO simultaneous methanolysis and esterification	Autoclave	300	5	60	4:1		98.3	[71]
Zeolite Steel furnace slag	WCO methanolysis	Batch stirred reactor (500 rpm)	62	3	240	12:1		96	[72]

*Catalyst content

The obtained material had a poorly developed surface area (about 10 m^2 g^{-1}), but showed respectable activity, probably due to residual Na_2O from the synthesis process (washing step until neutral pH was not applied). Perhaps the active Na_2O loaded in this way can be also the explanation for a gradual decrease in the catalyst activity in 3 repeated cycles, due to probable Na_2O leaching from the catalyst into the reaction mixture. A similar synthesis route was applied for kaolin clay transformation into LTA zeolite, but in this case, there was no need for acid treatment due to the absence of interfering metals in the starting clay (*e.g.*, Ca, Fe, *etc.*) [73]. It should be also added that after the hydrothermal synthesis step, thorough washing of the resulting material was carried out. Although the catalyst with the longest investigated ageing time of 48 h proved to be the most active, since the conversion yield did not change significantly with prolonging the ageing duration over 24 h, this time period was adopted as optimal. Statistical optimisation of reaction parameters by using the Box-Behnken design revealed optimal reaction conditions in methanolysis of triolein that were somewhat harsh (catalyst loading of 72 wt.%, methanol to oil molar ratio of 37:1, and reaction time of 2.4 h). Kaolin clay was also a starting material for the synthesis of zeolite Y, which was used as an HY zeolite catalyst for the esterification of oleic acid [74]. The Si/Al ratio in the prepared catalyst was 3.1, unlike zeolite X with the Si/Al ratio lower than 1.5, indicating the formation of a more catalytically active and stable form of faujasite (zeolite Y) [75]. Interestingly, the synthesized HY zeolite catalyst from kaolin had similar composition and morphological characteristics as a commercial HY zeolite catalyst. In addition, the synthesized HY zeolite catalyst showed better performance under very mild esterification conditions than the commercial HY zeolite (oleic acid conversion was about 84 and 68 % achieved in 45 min, respectively).

FAU-type zeolite was prepared by using Irish shale rock and tested as a catalyst in the esterification of oleic acid [76]. The catalyst was prepared in a common manner combining acid leaching, alkaline fusion, and hydrothermal treatment.

All these steps were experimentally optimized yielding the optimal mixing time of 3 h, ageing time of 18 h, and hydrothermal time of 24 h. Under these optimized synthesis conditions, a well-developed specific surface area was obtained (571 $m^2 g^{-1}$). The catalytic activity was similar to that of a commercial zeolite Y under the same reaction conditions. In the same manner another FAU-type zeolite catalyst was prepared and additionally modified with precious metals (Co, Ni, and Pt) by using the incipient wetness method to enhance the catalyst activity under continuous reaction conditions [57]. Under the same mild reaction conditions of oleic acid esterification with ethanol in a batch process, the Co-Ni-Pt-FAU zeolite catalyst was superior to the H-FAU zeolite catalyst, achieving the maximum obtained conversion of 93 *vs*. 78 %, respectively. The comparison was also made under continuous reaction conditions in a fixed-bed reactor indicating the Co-Ni-Pt-FAU zeolite catalyst superior again, achieving the conversion of 89 *vs*. 75 %, respectively, at the liquid hourly space velocity of 0.5 h^{-1}.

3. 3. 1. Zeolite-based catalysts originating from coal fly ash

Investigation of fly ash is becoming attractive in recent years due to the search for eco-friendly procedures for zeolite synthesis. Coal fly ash is a product of coal combustion that is composed of fine particles that are driven out of coal-fired boilers together with exhaust gases. Therefore, zeolites originated from this source belong to the group of zeolitic materials obtained from waste but are described in a separate subsection in the present review paper due to the high interest of researchers and engineers in this zeolite type in recent years. Attention to fly ash as a feedstock for zeolites synthesis was raised due to its aluminous and siliceous nature. Three key steps are included in the common production procedure of zeolite from fly ash *via* the alkali hydrothermal method [78]. Fly ash is first dissolved to produce Si^{4+} and Al^{4+} species in the solution followed by condensation of these ionic species to form aluminosilicate gel, which is then crystallized in the third step into desired zeolite crystals. Generally, the obtained catalysts showed excellent activity under mild reaction conditions (10) and respectable stability (11). They exhibited similar morphological characteristics as other waste-based catalysts, due to the similar feedstock composition and synthesis routes, meaning a medium or poorly developed specific surface and a mesoporous structure (Table 8).

Table 10. Review of reaction conditions when using zeolitic materials obtained from fly ash as catalysts/catalyst supports

| Catalyst designation | Feedstock | Reactor type | Optimal reaction conditions | | | | Yield (con-version), % | Ref. |
			$T /$ °C	CC*, wt.%	$t /$ min	Alcohol to oil molar ratio		
Zeolite Coal fly ash zeolite, sodalite type	Soybean oil methanolysis	Batch stirred reactor (300 rpm)	65	4	120	12:1	95.5	[79]
FA/K-X Fujasite zeolite type from South African class F fly ash	Sunflower oil methanolysis	Batch stirred reactor (600 rpm)	65	3	480	6:1	83.5	[86]
Li/NaY Zeolite from Chinese coal fly ash	Castor oil ethanolysis	Batch stirred reactor (400 rpm)	75	3	160	18:1	98.6	[85]
CaO/ZM$_{FA}$ Lignite coal fly ash (Serbia) CaO from eggshell	Sunflower oil methanolysis	Batch stirred reactor (850 rpm)	60	4	120	12:1	(96.5)	[29]
SC-Na Zeolite from Korean coal fly ash	Soybean oil methanolysis	Batch stirred reactor (200 rpm)	50	2	180	5 $cm^3 g^{-1}$ oil	95	[84]
Zeollite X Indian F-type coal fly ash	Soybean oil methanolysis	Batch stirred reactor	65	3	480	6:1	81.2	[83]
AZ-KX zeolite X zeolite from fly ash	Mustard oil methanolysis	Batch stirred reactor	65	5	420	12:1	(84.6)	[81]
Hydroxy sodalite South African coal fly ash	Maggot oil methanolysis	Batch stirred reactor	60	1.5	90	15:1	86	[82]
CaO/FA-ZM Lignite coal fly ash (Serbia) CaO from eggshell	Sunflower oil methanolysis	Batch stirred reactor (850 rpm)	60	6	30	6:1	(97.8)	[42]
Kaliophilite Circulating fluidized bed fly ash (Inner Mongolia, China)	Canola oil methanolysis	Batch stirred reactor	85	5	360	15:1	99.2	[87]

*Catalyst content

Table 11. Review of stability/reusability of zeolite-based catalysts

Catalyst designation	Reactor type	Catalyst stability/reusability	Ref.
Mg/clinoptilolite	Stirred batch reactor	At least 5 cycles	[48]
K-MAP	Pressured stirred batch high power density (microwave system) reactor	At least 3 cycles (catalyst was washed with methanol 3x and calcined at 450 °C for 2 h)	[62]
7 % Mo-NaBeta	Stirred autoclave	Conversion decreases by 18 % after the first cycle, and after that for the next three remains stable.	[63]
0.25 HPW/ZIF-67	Autoclave	6 cycles (conversion of 91.3 %) After washing with n-hexane and methanol efficiency was restored to 94.6 %	[67]
35 % CaO/zeolite	Microwave reactor	After 2nd cycle yield felt to18.3 %.	[61]
HMCM-36	Stirred batch reactor	At least 4 cycles (Only washing with methanol and drying at 70 °C)	[65]
AZ-KX zeolite	Stirred batch reactor	After 3rd cycle yield has significantly dropped (the catalyst was washed with methanol and calcined at 300 °C for 2 h)	[81]
FA/K-X	Stirred batch reactor	After 2rd cycle yield dropped ≈ 12 %	[86]
1:1-Li/NaY	Stirred batch reactor	In 5 cycles yield dropped from 98.6 to 80 % and after calcination restored to 91.6 %	[85]
SC-Na	Stirred batch reactor	At least 3 cycles	[84]
2D Na/ITQ-2	Stirred batch reactor	At least 4 cycles (yield >94 %)	[64]
Ba/CAN	Stirred batch reactor	Yield drops in 2nd cycle from 98 to 46 %. Regeneration is possible with calcination at 500 °C for 6 h.	[77]
K/zeolite	Stirred batch reactor	Yield drops in the 2nd and 3rd cycles from 81.9 to 62.7 % and 52.3 %, respectively.	[47]
K_2O/zeolite	Stirred batch reactor	At least 4 cycles	[50]
Ni/zeolite	Stirred batch reactor	Yield drops from 82.7 to 73.3 %, from the first to the third cycle, respectively	[70]
Zeolite	Autoclave	Yield drops from 98.3 to 58.93 %, from the first to the third cycle, respectively	[71]
CaO/FA-ZM	Stirred batch reactor	There was almost no decline in catalyst activity in 5 cycles (FAME content from 99.2 to 97.9 %) without any pretreatment	[42]

A neat sodalite form of zeolite was synthesized and used for methanolysis of soybean oil [79]. Fly ash from a Brazilian thermal power plant (Rio Grande do Sul state) had a SiO_2 content higher than 60 wt.% suitable for zeolite synthesis by a common route with 24 h crystallisation, washing until pH of 9, and a somewhat longer ageing period of 6 days. The calculated Si/Al ratio was 3, which places the obtained zeolite in the group of medium silica zeolites (Y, Ω, mordenite, *etc.*) [80]. The zeolite proved to be very catalytically active achieving a biodiesel yield of 95.5 % in 2 h under mild reaction conditions. In another study [81] several zeolite X and A catalysts were synthesized and compared in the methanolysis of mustard oil.

The Si/Al ratio was carefully controlled by the addition of adequate amounts of $NaAlO_2$ in order to avoid the formation of another, undesirable, zeolitic phase. So, Si/Al ratios lower than 2 and equalling to 2 were achieved to favour the formation of zeolite A and zeolite X, respectively. A preference was given to the zeolite X series of catalysts due to much higher specific surface areas as compared to zeolite A catalysts (over 160 $m^2\ g^{-1}$ *vs.* about 24 $m^2\ g^{-1}$, respectively).

Among zeolite X catalysts, the acid-treated ion-exchanged (K^+) catalyst showed the highest conversion explained by the increase in base strength upon ion-exchange. Still, even at optimal synthesis conditions this catalyst showed limited performance, especially at the introductory phase of the reaction, which lasted a long time (4-5 h) at a slow reaction rate indicating diffusion limitations [81]. This problem was not present to such an extent in the reaction catalysed by hydroxy sodalite zeolite [82]. Perhaps the reason for such performance is the obtained 100 % relative crystallinity in the catalyst. Both studies were conducted under mild reaction conditions, using used mustard oil and maggot oil with a similar acid value, respectively. The maximal obtained biodiesel yields were similar, but in the second case, it was reached much faster *i.e.*, in 1.5 h needed to reach the reaction equilibrium, which was about 4.6-fold faster than in the first study. A hydroxy sodalite zeolite catalyst was obtained from coal fly ash collected from a power plant in South Africa by using the common synthesis procedure with a relatively longer hydrothermal process time of 72 h [83]. A similar maximum biodiesel yield, as in the previous two studies, was obtained (about 80 %) by using neat hydroxy sodalite zeolite [83]. It is interesting that under very mild conditions of hydrothermal crystallization (90 °C and 8 h), zeolite X with a highly developed specific surface area of 727.2 $m^2\ g^{-1}$ was obtained [83].

A series of zeolite-like materials were obtained by acidification and subsequent alkali and alkaline earth metal hydroxides activation of coal fly ash from Korea [84]. In general, using such a synthesis route from coal fly ash, materials with a zeolite structure can be obtained, especially for example the form of a cancrinite-sodalite group of zeolite-like material (vishnevite type) [29, 42]. The study showed that the activity of the obtained catalysts decreased in the following order: Na activated > Ca activated > K activated >>> neat acid-treated fly ash, whereas the last one showed negligible activity. These results were probably obtained according to the order of theoretical basicity of the synthesized catalysts, since they all had approximately equal amounts of deposited metal oxides (about 60 wt.%). Interestingly, transesterification at the reaction temperature of 50 °C proved to be as good as at the commonly applied temperature of 60 °C. However, at the higher temperature, the reaction rate was slightly faster in the introductory stage, so eventually the reaction equilibrium was reached for both temperatures in the third hour. Also, the reactor stirring rate was found to be best at 200 rpm in the investigated range of 50-600 rpm. This is certainly related to the diffusion limitations and the surface morphology of the catalyst, which was not investigated so this phenomenon cannot be explained with certainty. Loading of lithium by co-precipitation on hydrothermal and microemulsion-assisted synthesized NaY zeolites was also investigated [85]. The best catalyst (NaY zeolite/Li_2CO_3 molar ratio = 1/1 and calcination temperature of 750 °C) achieved remarkable activity and stability. The yield of 98.6 % of fatty acid ethyl esters (FAEEs) was achieved under mild reaction conditions in 2 h of reaction. Moreover, the catalyst was proved to be very air tolerant, which is one of the main disadvantages of heterogeneous base catalysts, as well as to be recyclable. The activity of three similar catalysts loaded with Li was compared and a decline in activity was found regarding the support in the following order: NaY zeolite, Al_2O_3, and SiO_2. All three catalysts had a very high basic strength of 15<$H\_$<18.4, but the obtained differences in activity lay in differences in BET surface area and basicity, which were consistent with the activity shown. It was found out that the best catalyst was not the one with the highest Li load, nor the one calcined at the highest temperature. The neat NaY zeolite had a highly developed specific surface area (429 m^2 g^{-1}) that, as expected, decreased with the loading of Li. Interestingly, the 3:1 Li/NaY catalyst had a specific surface area of only 1.6 m^2 g^{-1}. The same pattern of the specific surface area decreases from 193 m^2 g^{-1} to 18 m^2 g^{-1}, following the increase in the calcination temperature from 550 °C to 950 °C. The catalyst with the highest Li load had the highest total basicity, as expected, but the catalyst with a more suitable surface morphology was more active although it contained a lower amount of Li. It is necessary to mention that the difference in basicity was not large and that is why the morphology came to the fore.

A faujasite zeolite material synthesized from a South African class F fly ash was ion-exchanged with K to obtain a potent catalyst for sunflower oil methanolysis [86]. The catalyst was prepared according to the conventional hydrothermal synthesis procedure and the alkali metal (K^+) ion exchange. The obtained material had a finely developed surface area of 257 m^2 g^{-1} (starting fly ash had only 2 m^2 g^{-1}) and a considerably high basic strength of 15<$H\_$<18.4. However, under mild reaction conditions, the catalyst did not show exceptional activity, as in 8 h of reaction the biodiesel yield was 83.5 %. Additionally, even after 24 h, the yield was not much higher. The reason for the average performance of the catalyst might be the unavailability of some of the catalytically active centres dispersed in, probably dominant, small-diameter pores for large organic molecules in the reaction mixture.

A lignite coal fly ash-based zeolite was used as a support for loading chicken eggshell calcium oxide using two synthesis routes in order to obtain sustainable and green catalysts [29,42]. The first route involved a hydration-dehydration method as the last step of the synthesis [42], while the second route used ultrasonic dispersion in an alcoholic suspension [29]. Naturally, both synthesis procedures had calcination as a final catalyst activation step. The cancrinite-sodalite zeolite-like material (vishnevite type) was synthesized by the common procedure: calcination - acidification - alkali activation - hydrothermal crystallization. The fly ash obtained from a Serbian thermal power station was converted into a zeolite-like material using, for the first time, a rotating miniature autoclave reactor system [29]. The reactor allowed adequate agitation by rotating the whole reaction mixture, instead of contact mixing by a stirrer. In this way, significant savings in time and energy were achieved along with obtaining a more homogeneous product. For instance, in the autoclave system set-up, the hydrothermal crystallization step lasted only 4 h. The best catalysts prepared by using both routes had similarly developed specific surface areas of about 20 m^2 g^{-1} and relatively high

basicity. The 50 % CaO/zeolite catalyst showed remarkable activity under mild reaction conditions (*e.g.*, methanol to oil molar ratio of 6:1 proved to be most adequate) and in only 0.5 h the equilibrium FAME content was 97.8 %. It was shown once again, as in the study by Li *et al.* [85], that only one parameter of the catalyst does not decisively determine its activity, but the synergy of several key parameters. The 20 % CaO/zeolite catalyst was more active than the neat eggshell-based CaO despite its almost 4.5-fold higher basicity. Adequate surface texture and morphology combined with finely dispersed base centres were key features for determining the catalytic activity. The specific surface area of neat the CaO was 15-fold lower, while its porosity was 55 %, which is significantly lower than 86.5 % determined for the CaO/zeolite catalyst. The spent catalyst had signs of deposition of organic molecules from the reaction mixture, although it was proven not to be significant, as confirmed by the maintenance of high activity in 5 consecutive cycles, without any catalyst pretreatment.

A circulating fluidized bed fly ash from a laboratory was used to synthesize kaliophilite catalyst *via* a facile and low-energy two-step process: fabrication of an amorphous fly ash geopolymer and hydrothermal transformation of the geopolymer into kaliophilite [87]. The kaliophilite catalyst exhibited a poorly developed surface area (3.5 m^2 g^{-1}), but the average pore diameter of 20.9 nm and the majority of mesoporous pores promoted the catalytic activity for the reaction involving relatively large organic molecules so that a high biodiesel yield and short reaction induction period were achieved confirming these favourable morphological characteristics.

4. REACTION MECHANISMS OF TRANSESTERIFICATION CATALYZED BY ZEOLITE CATALYSTS

Common production of biodiesel implies transesterification of TGs from vegetable oils, oily waste, or animal fats with alcohol in presence of a catalyst to produce fatty acid alkyl esters (FAAEs) and glycerol. The reaction is three-staged, but the overall reaction can be represented by Figure 3. Before obtaining three FAAE molecules, the intermediates diacylglycerol and monoacylglycerol are formed and then broken up in successive reactions.
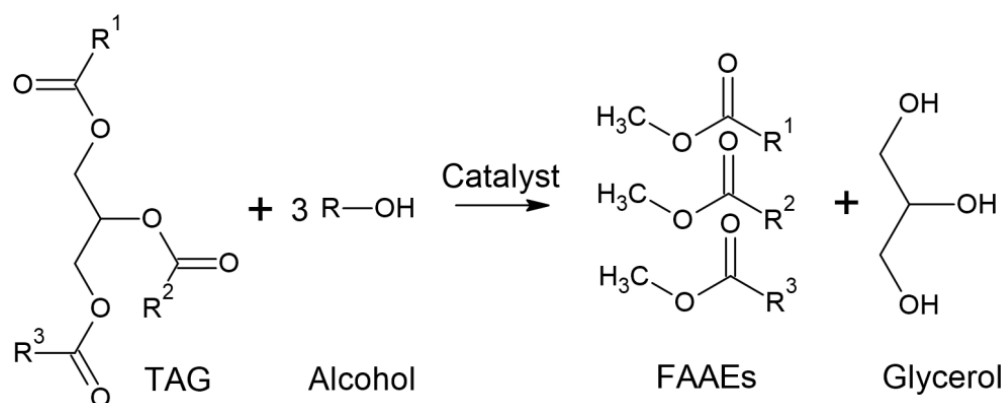

Figure 3. General scheme of transesterification reaction

Heterogeneous catalytic production of biodiesel follows similar principles to those of homogeneous catalysis. In the base-catalysed reaction, the first and main step is to create nucleophilic alkoxides from the present alcohol that attack the electrophilic part of the carbonyl group in TGs, whilst in the acid-catalysed process the carbonyl group in TAGs is protonated and then the present alcohol attacks the protonated carbon to produce a tetrahedral intermediate species [3].

Detailed mechanisms of reactions catalysed by zeolite catalysts have been proposed by several authors [3,63,67,79,88]. Different structural, physical and chemical properties of zeolite catalysts, whether with basic, acid, or bifunctional acid-base active sites, caused somewhat different explanations of the mechanisms.

Figure 4 presents a mechanism proposed for rice bran oil transesterification using a NaBeta zeolite supported-Mo catalyst [63]. First, triglyceride molecules are adsorbed onto the catalyst surface, and intermediate (step 1) species are obtained from the unpaired electron from the oxygen atom of C=O in triglyceride, bond with molybdenum oxide species. Further, carbocation (step 2) is produced due to the transfer of the electron pair from the oxygen atom to the carbon atom within the C=O bond. Next, a nucleophilic reaction takes place where methanol and the intermediate from step 2

form new intermediate species (step 3) in which a new intermediate compound (step 4) is obtained by H$^+$ transfer. Breaking the C-O bond in C-OH-CH$_2$ leads to the separation of a diglyceride (DG) molecule. Additionally, C=O group was produced when an electron pair of oxygen atom was transferred into C-O single bond of Mo-C-O whereby a new intermediate compound (step 5) is formed. Finally, heterolysis of the electron pair in the Mo-O bond promotes the formation of a FAME molecule and regeneration of the catalyst, thus finishing one reaction cycle.
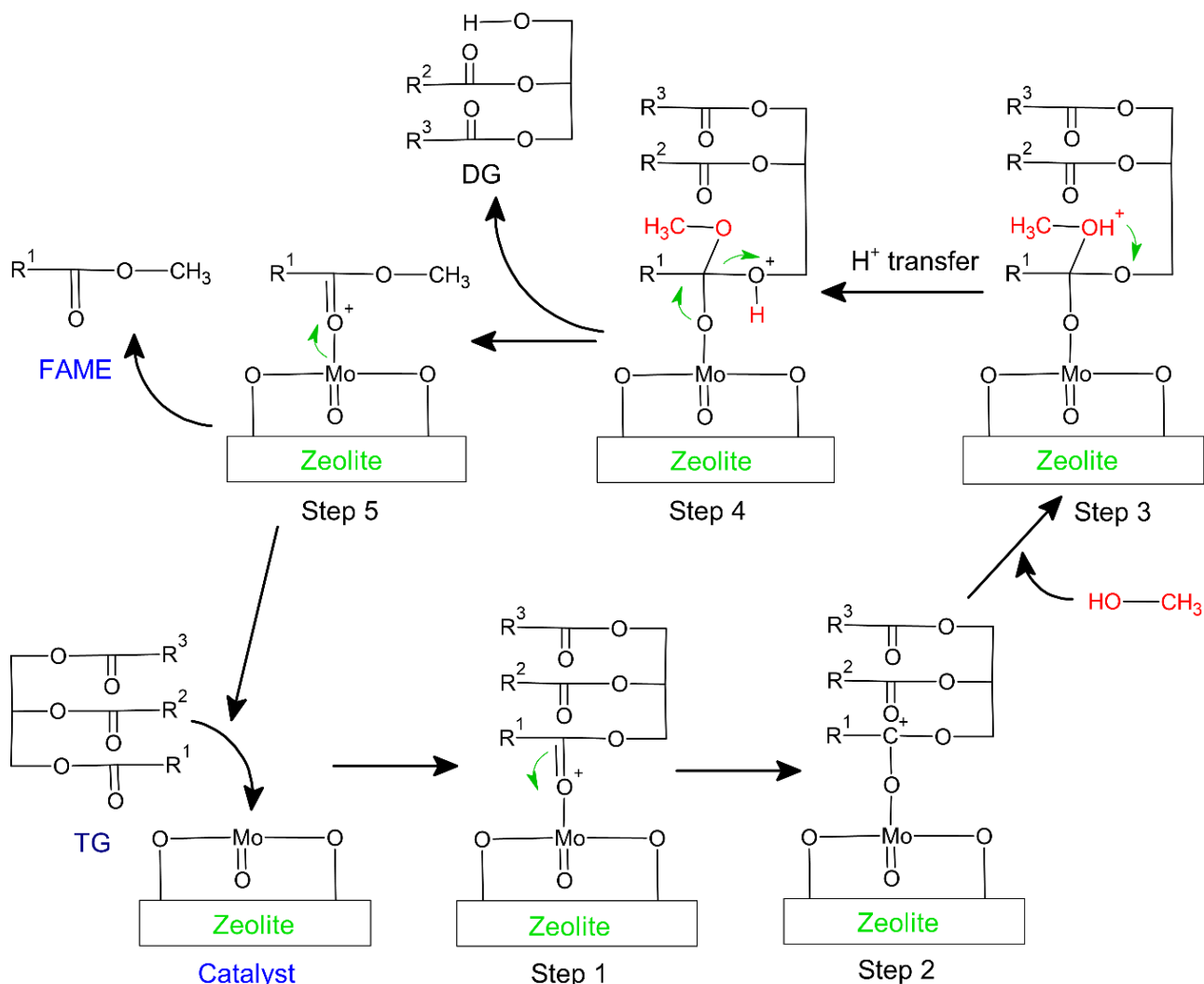

Figure 4. Proposed mechanism of transesterification catalyzed by a Mo/zeolite catalyst [63]

Si-O-Na groups in the structure of a sodalite zeolite catalyst act as active sites for the transesterification reaction [79]. The proposed mechanism (Figure 5) for this zeolite catalyst action follows a similar pathway as for homogeneous base catalysts [3]. In the first step, methanol is adsorbed onto the surface and catalytic active species (methoxide anion) are produced. The second step is the nucleophilic attack of methoxide anion on the carbonyl carbon of triglyceride and the formation of tetrahedral intermediate species. The third stage is unstable intermediate rearrangement forming a FAME molecule. Finally, deprotonation of the catalyst is happening, thus regenerating the catalytically active species. This cycle was repeated two more times to yield glycerol and three molecules of biodiesel.
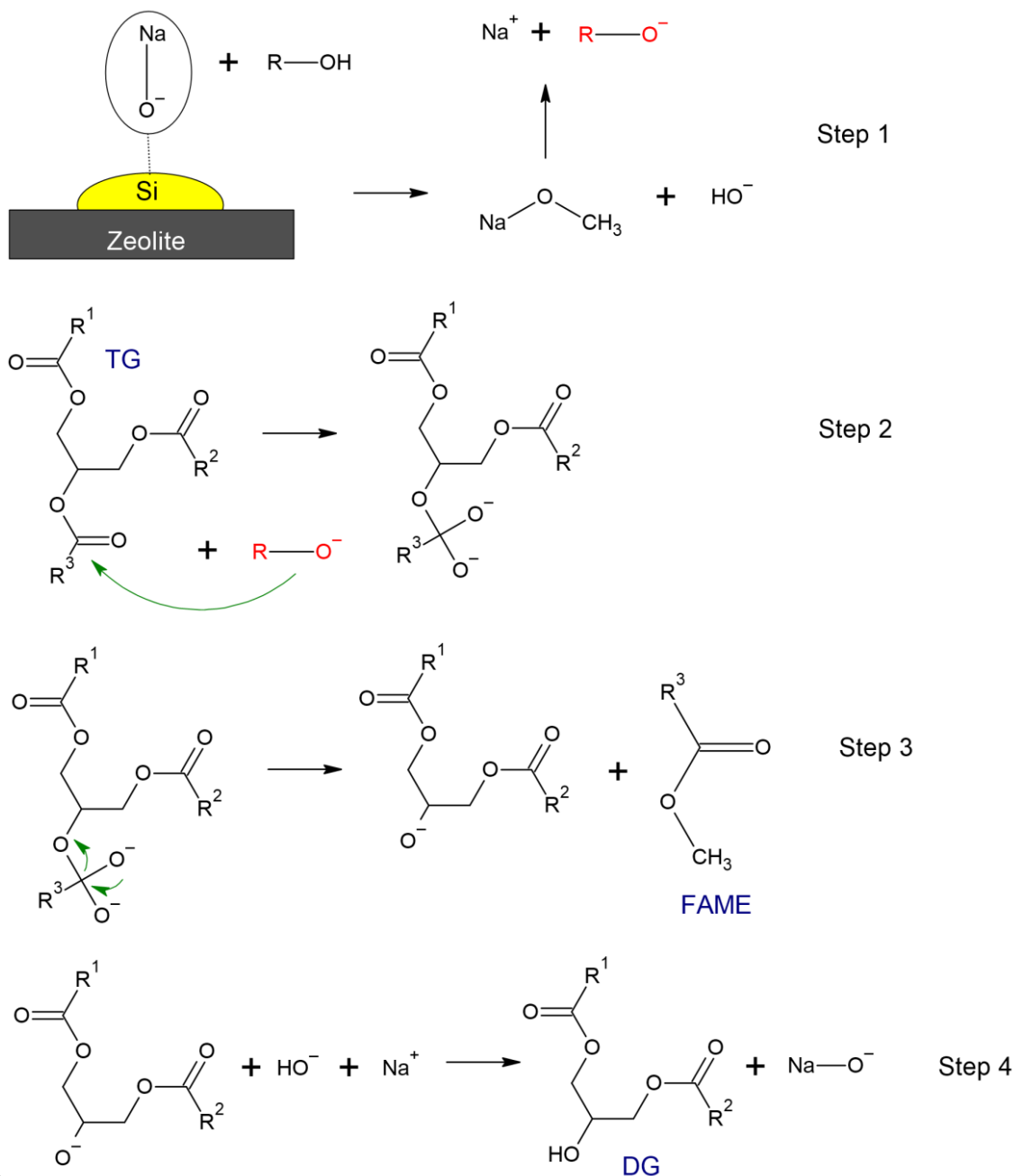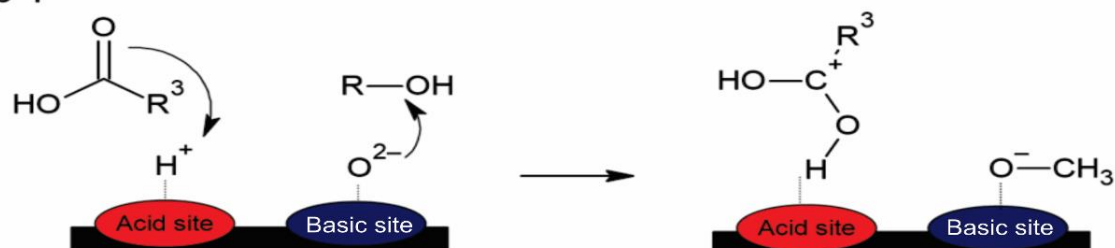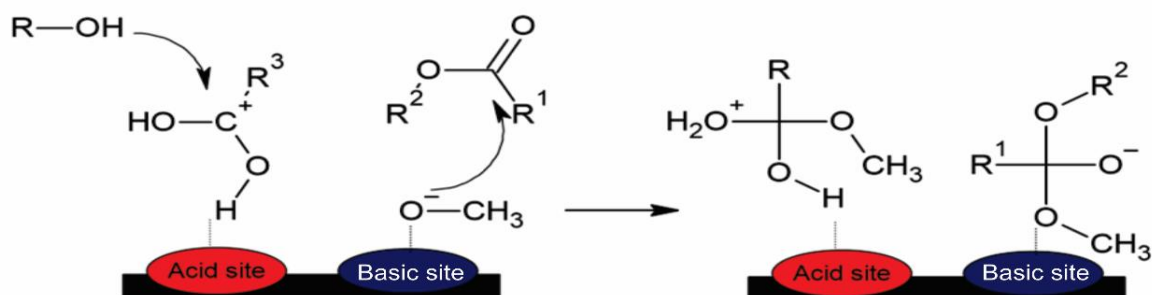
Figure 5. Transesterification reaction mechanism using sodalite zeolite catalyst [79]

Figure 6 presented pathways for the acid-base catalysed biodiesel production using a zeolite-based catalyst. The presence of acid and base catalytic sites allows the catalyst to perform simultaneous esterification and transesterification reactions [88]. In acid-catalysed pathways carbocation is initially formed by adsorption of the carbonyl group of FFA on the acid site on the catalyst surface. In the step 2, a nucleophilic attack by methanol on the carbocation leads to the formation of tetrahedral intermediate species. Breaking the O-H bond and desorption of the hydroxyl group from the catalyst surface in the final 3rd step, produces a FAME molecule. The base-catalysed pathways start with the formation of a methoxide anion as a result of methanol adsorption onto the basic catalyst sites. The resulting methoxide anion as a highly reactive nucleophilic species, attacks the carbonyl carbon in triglycerides to form another tetrahedral intermediate species. The third step involves desorption of alkyl triglycerides from the catalyst surface, *i.e.*, formation of a FAME molecule, after breaking the C-O bond.
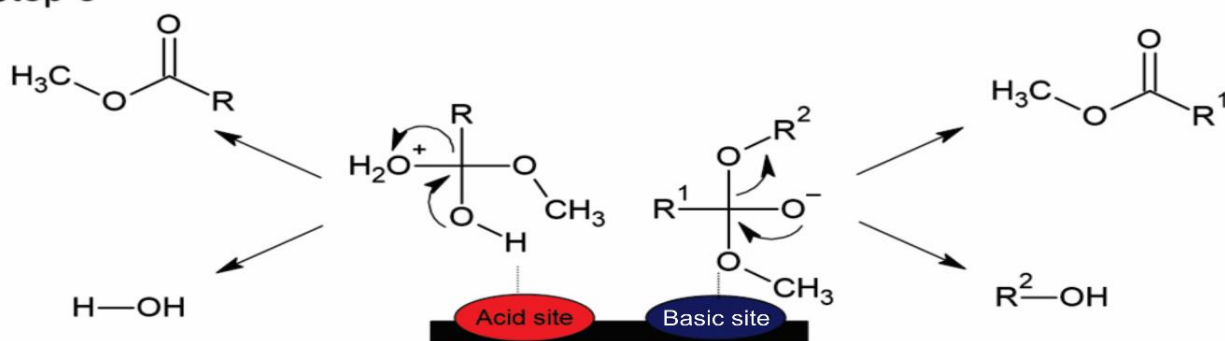
Figure 6. Proposed mechanism of bifunctional acid-base transesterification [88]

Cheng *et al.* [67] suggested a reaction mechanism where a bifunctional HPW/ZIF-65 zeolite-based catalyst exhibited three kinds of catalytically active sites: Brønsted acid sites, and Lewis acid and base sites. Protons of -NH and HPW represented Brønsted acid sites, coordinatively unsaturated cobalt cations represented Lewis acid sites, while N⁻ extremities of imidazole ligands acted as Lewis base sites. As presented in Figure 7, the carbonyl oxygen of the fatty acid is adsorbed on the Lewis acid site (L⁺) to form a carbocation as the hypothesis is that these sites mainly catalyse FFAs esterification. Then alcohol starts the nucleophilic attack to the carbocation to produce a tetrahedral intermediate, which is unstable and decomposes to FAME, water molecule, and L⁺. The transesterification reaction is catalysed on Lewis base sites (L⁻). It starts with the contact of adsorbed alcohol on active sites (N⁻ extremities of imidazolate ligands) and TG to form an oxygen anion. A tetrahedral intermediate is, then, produced in the nucleophilic attack of oxygen anion to TG. The unstable tetrahedral intermediate is in the second step decomposed to FAME and DG. This process is repeated to DG and monoglycerides (MG) to finally form three molecules of FAME. The Brønsted acid sites can act bifunctionally, as they can catalyse FFA esterification and TG transesterification simultaneously. A carbocation is formed in the reaction of the proton from -NH and protonated HPW and the carbonyl group of TG. Then, the nucleophilic attack of alcohol to the carbocation forms a tetrahedral intermediate, which is decomposed to another proton and products.
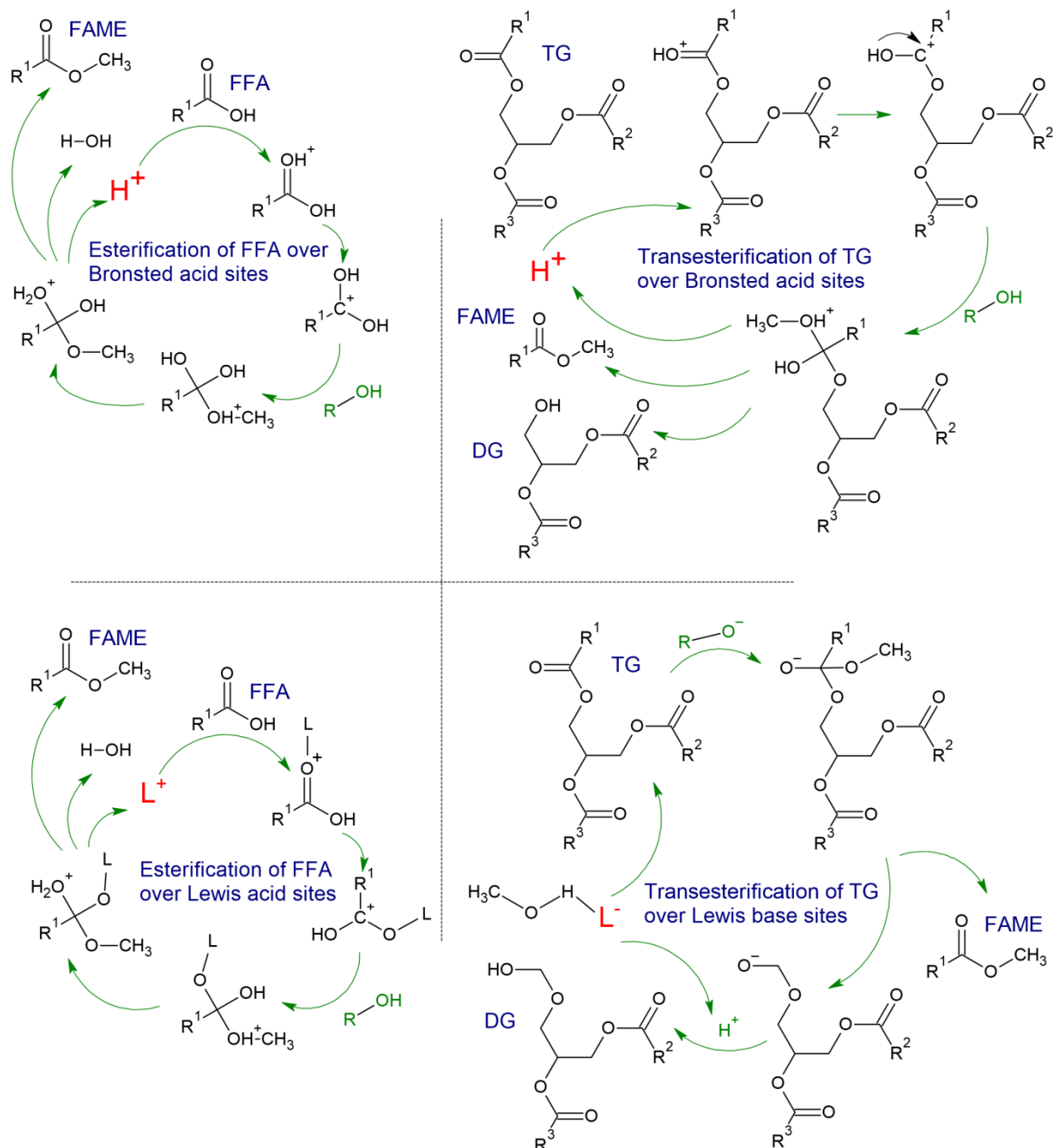
Figure 7. Proposed mechanism of bifunctional zeolite-based catalysis through Lewis acid and base sites and Brønsted base sites [67]

5. STABILITY OF ZEOLITE-BASED CATALYSTS

Most studies of zeolite-based catalysed biodiesel production were performed under batch reaction conditions, so that the catalyst stability can be investigated by determining the catalyst activity in repeated consecutive reaction cycles. The spent catalysts were used in consecutive cycles either without any treatment, subjected to some regeneration procedure, or simply washed in some solvent. Catalyst regeneration was performed in some studies by recalcination [62,81,77,85], while polar (such as methanol) [65,67,81] or non-polar (such as n-hexane) [67] solvents were used for rinsing. A great diversity of zeolite structures in the studied catalysts, as well as different catalytically active species, led to a colourful picture regarding the stability of catalysts. Some materials managed to maintain high activity in six consecutive cycles, while others had a significant decrease in activity already in the second cycle. Furthermore, maintaining high activity in six repeated cycles is the best-achieved performance reported [67] among the reviewed

literature, but this result should be taken with caution as in many studies the maximum stability of the catalyst was not determined, despite the good performance of the material in several cycles [48,50,62,64,65,84].

The stability issue of heterogeneous catalysts exposed to air is one of the most important characteristics for evaluating the catalyst quality. A Li/NaY zeolite catalyst was proved to be very tolerant to air exposure, as after 10 days of exposure the FAEE yield dropped from the initial 98.6 to 92.6 % [85]. In a study of the effects of washing solvents [48] between cycles, methanol showed slightly better results than distilled water as in 5 consecutive cycles the biodiesel yield decreased from 98.7 to 92 % and 94.5 % when using water and methanol for rinsing, respectively. A green catalyst of a lignite fly ash-produced zeolite supporting CaO (from chicken eggshells) showed great reusability in five investigated consecutive cycles without any pretreatment achieving a minor decline in activity (the FAME content decreased from 99.2 to 97.9 %) [42]. It is interesting, that such high activity is preserved despite the rather high leaching of Ca into the FAME phase (range of 1170 mg kg^{-1} to 630 mg kg^{-1}). It should be noted that CaO impregnation on the zeolite support stabilized the catalyst since, under the same reaction conditions, Ca leaching from the neat CaO catalyst was 4-fold higher. In this study as well, the deposition of organic molecules from the reaction mixture on the catalyst surface was observed, but in this case, intriguingly, it seems rather not affecting the catalyst activity. In this case also attention should be paid to the purification of the obtained biodiesel to meet the strict standards (Ca + Mg <5 ppm [89]). A pillared acid HMCM-36 zeolite catalyst proved to be very stable, in four repeated cycles only washed with methanol without a significant decline in activity [65]. A K-form of zeolite MAP was highly active in three repeated cycles (yields from 96 to 94 %) along with a turnover frequency of 202 h^{-1}, with methanol washing and recalcination after each cycle. With the same reactivation procedure, a K/fly ash-originated zeolite X catalyst was also highly active in three cycles, after which the activity significantly dropped. Recalcination was used as a method for reactivation of the spent K$_2$O/zeolite catalyst before each run successfully performing in four consecutive cycles, after which the activity dropped [50]. This finding is explained by morphology changes in the material, such as crystal agglomeration, and a consequent decrease in the catalytic surface area, during the consecutive heating process. The excellent recyclability is displayed by a two-dimensional Na/ITW-2 zeolite catalyst with hardly any changes in activity after four consecutive cycles (the catalyst was washed with ethanol and ethyl acetate) [64].

Without any pretreatment the activity of a Li/NaY zeolite catalyst gradually declined from 98.6 % (FAEE yield) to about 80 %, but after recalcination, the catalyst regained its activity to the FAEE yield of 91.6 % achieved in the sixth cycle [85]. The XRD analysis showed that the reduction of the active component (Li$_4$SiO$_4$ and Li$_3$NaSiO$_4$) in favour of Li$_2$SiO$_3$ was responsible for the activity drop, recovering it by the reverse reaction during recalcination.

A bifunctional phosphotungstic acid-modified zeolite imidazolate framework (ZIF-67) catalyst has shown excellent stability in microalgal lipids esterification and transesterification [67]. The activity dropped by 7.2 % in six repeated cycles (still the conversion was up to 91.3 %) without any pretreatment. The reason for this slight decline in activity was found in the deposition of unrefined microalgal lipids into the pores of the material and the breaking of a small amount of W-O-N bonds resulting in the loss of active HPW. It is significant that after six cycles the activity was completely recovered only by washing with methanol and n-hexane [67].

Significantly lower stability was found in the use of a 35 % CaO/zeolite catalyst, which activity decreased from cycle to cycle, to be negligible in the fourth cycle [61]. In this study, a commercial ZSM-5 zeolite was used as a support, while CaO was loaded by impregnation from an aqueous solution using calcium acetate. Similar CaO/zeolite catalysts were prepared in some other studies [29,42] by hydration-dehydration and ultrasound-assistant alcohol impregnation of CaO on fly ash-based zeolite carrier. The difference in precursors and the synthesis methods probably affected the lower stability and recyclability of the former catalyst [61], especially considering a report that calcium acetate was not shown to be the best precursor for achieving stability of CaO-based catalysts [90]. A high drop in conversion efficiency of soybean oil to biodiesel from 98 % to about 46 % was reported in the second cycle in 1.5 h of reaction catalyzed by a diatomaceous earth cancrinite-type zeolite catalyst [77]. This result is rather surprising considering the presented x-ray diffraction, infrared spectrometry, and electronic microscopy analyses, showing imperceptible differences between the fresh and spent catalyst, except occasional smaller agglomerates evolved on the surface of the spent material. Similarly, a gradual decline in the biodiesel yield from cycle to cycle was reported in a study attempting simple regeneration of a

K/natural zeolite catalyst by washing in n-hexane [47]. The reduction in catalyst activity was explained by the leaching of active species into the reaction medium. The same explanation for the catalyst activity decline was provided in the case of a waste-based zeolite carrier impregnated with Ni [70] and a neat zeolite catalyst obtained from geothermal solid waste [71]. Interesting behaviour was shown by a NaBeta zeolite-supported molybdenum catalyst [63], which showed a relatively good activity in the first cycle, followed by a decline in activity of 18 % in the second cycle and remaining at a constant level in the other three consecutive cycles. This behaviour is explained by the deposition and binding of organic molecules from the reaction mixture to the surface of the catalyst in the first cycle, which did not continue in the subsequent cycles.

In general, it can be concluded that the stability of zeolite-based catalysts has not been comprehensively investigated, changes in the materials occurring during the course of the reaction have not been analytically assessed and discussed in sufficient detail, as well as insufficient attention has been paid to optimization of the catalyst regeneration and exploring the maximal reusability of the catalysts. In particular, it is necessary to conduct research on the stability of these catalysts under industrially more favourable continuous process conditions.

6. QUALITY OF THE OBTAINED BIODIESEL

The use of zeolite-based catalysts produced biodiesel of high quality [48,63] according to the standards (ASTM D-6751 [91] and EN 14214[89]), contrary to some other prominent heterogeneous catalytic materials, such as CaO-based catalysts, in which case the obtained biodiesel has problems meeting the standard due to Ca leaching [3]. For example, methanolysis of high-density (0.959 kg dm^{-3} [92]) castor oil catalysed by a KOH/natural zeolite resulted in biodiesel with a density that exceeds the standard value [46]. Biodiesel produced from WCO by catalysis with a Na-modified clinoptilolite showed a high cetane number of 64.5 and was in accordance with the limiting (Na + K) concentration of 2.4 mg kg^{-1}[48]. Biodiesel with a lower cetane number (57.2) was obtained from castor oil catalysed by a Li/NaY catalyst [85]. Additionally, biodiesel density and viscosity were higher than the values prescribed by the standards due to the higher content of long hydrocarbon chains originating from the demanding feed oil. Other WCO-originated biodiesel obtained over a Ni/zeolite catalyst in a batch reactor [70] as well as over a KOH/clinoptilolite catalyst in a microreactor [45] met the European quality standard for density and kinematic viscosity. Waste lard-originated biodiesel, on the other side, exhibited a desirable FAME profile of 38.3 % saturated and 61.7 % unsaturated fatty acids [61]. Biodiesel obtained from microalgal oil showed a mixed methyl ester profile, where that obtained from the *Nannochloropsis oculata* oil contained a slightly higher amount of unsaturated fatty acids, in contrary to that obtained from the *Chlorela vulgaris* oil [53]. Amount of saturated methyl esters is a significant aspect of biodiesel since it determines its oxidative stability, while higher contents of unsaturated methyl esters make biodiesel suitable for usage in countries in colder regions, therefore, reducing the need for additives [53]. Canola oil-originated biodiesel blends (B10 and B20) satisfied the ASTM standard, moreover, the cetane numbers were high (64.3 and 67.2 for B10 and B20 blends, respectively) [87].

7. FUTURE PERSPECTIVES

Humankind has a real need to reduce GHG emissions into the Earth's atmosphere. Use of carbon-neutral biofuels is still imposed as one of the most immediate and effective approaches to the issue. Several readily available technologies are being developed to produce advanced biofuels. The commercial success of some of these fuels will depend on several issues, such as the production process complexity and consequently economy, availability and quality of the feedstock, and quality of the obtained fuel. Catalysis provides a versatile tool to resolve some of these issues by controlling the process reactions. For example, catalysts can simplify processes, reduce reaction time, and/or improve the resulting fuel quality.

Many studies on zeolite-based catalysts in recent years prove the high potential of these materials for efficient catalysis of biodiesel production reactions in the future. Zeolite-based catalysts show high catalytic activity, whether they possess basic, acid, or bifunctional acid-base active sites. This diversity enables these catalysts to successfully tackle oily feedstocks that have unfavourable characteristics for use in reactions with common heterogeneous, as well as homogeneous, catalysts. This is especially important from the point of view that most raw waste or inedible oils contain

large amounts of FFAs and moisture, which cause problems, particularly for base catalysts. Zeolite-based catalysts provide an additional benefit in the possibility to be obtained from waste raw materials, such as fly ash, a by-product of coal burning in thermal power plants, industrial slags, *etc*. This promotes the sustainability of biodiesel production since waste materials can be used both as oily feedstock in the reaction and as raw material to produce catalysts. Taking all this into account, catalysts based on zeolites, therefore, belong to the group of the most preferred heterogeneous catalysts for the transesterification or esterification reaction of TGs.

There are multiple synthesis methods with relatively simple control of the synthesis parameters providing zeolite-based catalysts with desirable characteristics required for such a reaction involving relatively large organic molecules. Regarding morphological and textural characteristics, these materials show high porosity and regularity of pores without pronounced bottlenecks, and exhibit large specific surface area and external surface area, with most of the pores belonging to the mesoporous region. Regarding the physical and chemical characteristics, they have a high concentration of basic and/or acidic active centres that are finely dispersed. These catalysts show significant stability in repeated reaction cycles as well as at high temperatures and elevated pressures.

Still, from the reviewed literature, It seems that good stability and retention of high long-term activity of zeolite-based catalysts demonstrated in batch processes have not been sufficiently investigated in continuous processes, where these positive properties of the material would be particularly important. Current research lacks implementation studies focusing on the intensification of the reactor operation with the use of these catalysts. Research investigating forced periodic reactor operation by periodic modulation of one or more inputs (*e.g.* reactants concentration, temperature, or flow rate) around a steady state operation shows promising state-of-the-art intensification approach [93,94], as well as the use of reactors in which mass transfer is intensified (microreactors, oscillatory baffled reactors, static mixers, *etc*.), are necessary to exploit the full potential of these catalytic materials.

Still, the main challenges for using zeolite-based catalysts will be the process scale-up, conducting large facility experiments, fine-tuning the materials for commercial applications and finding the synthesis routes that are more eco-friendly and less energy-demanding. Based on the presented encouraging results, it should be expected that more emphasis will be given to these topics in the future. Despite existing issues that remain to be solved, the huge variety of different zeolite-based catalysts, the possibility of obtaining them from waste, and the number of studies that dealt with this subject, confirm the promising potential of these materials as heterogeneous catalysts for biodiesel production in a sustainable manner at the industrial level. In this regard, important developments in the preparation of zeolites with increased acid/base active centres, porosity and external surface accessibility summarized in the present manuscript may pave the way for wider and more efficient use of crystalline-porous waste-based materials in biomass conversion processes.

REFERENCES

[1] Popović Z, Souček I, Marinković D, Jocić O. Viability of newly developed processes for catalytic conversion of bio-glycerin into various "green chemicals" and development opportunities for Serbia. *J Appl Eng Sci.* 2016; 14(3): 409-421 https://doi.org/10.5937/jaes14-9551.

[2] Baláž M, Boldyreva EV, Rybin D, Pavlovic S, Rodríguez-Padrón D, Mudrinic T, Luque R. State-of-the-Art of Eggshell Waste in Materials Science: Recent Advances in Catalysis, Pharmaceutical Applications, and Mechanochemistry. *Front Bioeng Biotechnol.* 2021; 8: 612567 https://doi.org/10.3389/fbioe.2020.612567.

[3] Marinković DM, Stanković MV, Veličković AV, Avramović JM, Miladinović MR, Stamenković OO, Veljković VB, Jovanović DM. Calcium oxide as a promising heterogeneous catalyst for biodiesel production: Current state and perspectives. *Renew Sustain Energy Rev.* 2016; 56: 1387-1408 https://doi.org/10.1016/j.rser.2015.12.007.

[4] Shan R, Lu L, Shi Y, Yuan H, Shi J. Catalysts from renewable resources for biodiesel production. *Energy Convers Manage.* 2018; 178: 277-289 https://doi.org/10.1016/J.ENCONMAN.2018.10.032.

[5] Narasimhan M, Chandrasekaran M, Govindasamy S, Aravamudhan A. Heterogeneous nanocatalysts for sustainable biodiesel production. *J Environ Chem Eng.* 2021; 9(1): 104876 https://doi.org/10.1016/J.JECE.2020.104876.

[6]   Mandari V, Devarai SK. Biodiesel Production Using Homogeneous, Heterogeneous, and Enzyme Catalysts via Transesterification and Esterification Reactions: a Critical Review. *Bioenergy Res.* 2021; 1: 1-27 https://doi.org/10.1007/S12155-021-10333-W.

[7]   Rizwanul Fattah IM, Ong HC, Mahlia TMI, Rahman MM, Silitonga AS, Rahman SMA, Ahmed A. State of the Art of Catalysts for Biodiesel Production. *Front Energy Res.* 2020; 8: 101 https://doi.org/10.3389/fenrg.2020.00101.

[8]   Wang YT, Fang Z, Zhang F. Esterification of oleic acid to biodiesel catalyzed by a highly acidic carbonaceous catalyst. *Catal Today*. 2019; 319: 172-181 https://doi.org/10.1016/J.CATTOD.2018.06.041.

[9]   Gebremariam SN, Marchetti JM. Biodiesel production through sulfuric acid catalyzed transesterification of acidic oil: Techno economic feasibility of different process alternatives. *Energy Convers Manage.* 2018; 174: 639-648 https://doi.org/10.1016/J.ENCONMAN.2018.08.078.

[10]   Andrade TA, Martín M, Errico M, Christensen KV. Biodiesel production catalyzed by liquid and immobilized enzymes: Optimization and economic analysis. *Chem Eng Res Des.* 2019; 141: 1-14 https://doi.org/10.1016/J.CHERD.2018.10.026.

[11]   Tran NN, Gelonch ME, Liang S, Xiao Z, Sarafraz MM, Tišma M, Federsel H-J, Ley SV, Hessel V. Enzymatic pretreatment of recycled grease trap waste in batch and continuous-flow reactors for biodiesel production. *Chem Eng J.* 2021; 426: 131703 https://doi.org/10.1016/J.CEJ.2021.131703.

[12]   Jeon Y, Chi WS, Hwang J, Kim DH, Kim JH, Shul YG. Core-shell nanostructured heteropoly acid-functionalized metal-organic frameworks: Bifunctional heterogeneous catalyst for efficient biodiesel production. *Appl Catal Environ*. 2019; 242: 51-59 https://doi.org/10.1016/J.APCATB.2018.09.071.

[13]   Mansir N., Teo SH, Rashid U, Saiman MI, Tan YP, Alsultan GA, Taufiq-Yap YH. Modified waste egg shell derived bifunctional catalyst for biodiesel production from high FFA waste cooking oil. A review. *Renew Sustain Energy Rev.* 2018; 82: 3645-3655 https://doi.org/10.1016/J.RSER.2017.10.098.

[14]   Jeon KW, Shim J-O, Cho J-W, Jang W-J, Na H-S, Kim H-M, Lee Y-L, Jeon B-H, Bae JW, Roh H-S. Synthesis and characterization of Pt-, Pd-, and Ru-promoted Ni-Ce$_{0.6}$Zr$_{0.4}$O$_2$ catalysts for efficient biodiesel production by deoxygenation of oleic acid. *Fuel.* 2019; 236: 928-933 https://doi.org/10.1016/J.FUEL.2018.09.078.

[15]   Tabandeh M, Cheng CK, Centi G, Show PL, Chen W-H, Ling TC, Ong HC, Ng E-P, Juan JC, Lan SS. Recent advancement in deoxygenation of fatty acids via homogeneous catalysis for biofuel production. *Mol Catal.* 2022; 523: 111207 https://doi.org/10.1016/J.MCAT.2020.111207.

[16]   Aboelazayem O, Gadalla M, Saha B. Valorisation of high acid value waste cooking oil into biodiesel using supercritical methanolysis: Experimental assessment and statistical optimisation on typical Egyptian feedstock. *Energy.* 2018; 162: 408-420 https://doi.org/10.1016/J.ENERGY.2018.07.194.

[17]   Farobie O, Leow ZYM, Samanmulya T, Matsumura Y. New insights in biodiesel production using supercritical 1-propanol. *Energy Convers Manage.* 2016; 124: 212-218 https://doi.org/10.1016/J.ENCONMAN.2016.07.021.

[18]   Khedri B, Mostafaei M, Safieddin Ardebili SM. A review on microwave-assisted biodiesel production. *Energy Sources A.* 2018; 41(19): 2377-2395 https://doi.org/10.1080/15567036.2018.1563246.

[19]   Fazril I, Shamsuddin AH, Nomanbhay S, Kusomo F, Hanif M, Ahmad Zamri MFM, Akhiar A, Ismail MF. Microwave-assisted in situ transesterification of wet microalgae for the production of biodiesel: progress review. *IOP Conf Ser: Earth Environ Sci.* 2020; 476(1): 012078 https://doi.org/10.1088/1755-1315/476/1/012078.

[20]   Patle DS, Pandey A, Srivastava S, Sawarkar AN, Kumar S. Ultrasound-intensified biodiesel production from algal biomass: a review. *Environ Chem Lett.* 2020; 19(1): 209-229 https://doi.org/10.1007/S10311-020-01080-Z.

[21]   Tan SX, Lim S, Ong HC, Pang YL. State of the art review on development of ultrasound-assisted catalytic transesterification process for biodiesel production. *Fuel.* 2019; 235: 886-907 https://doi.org/10.1016/J.FUEL.2018.08.021.

[22]   Stankovic M, Pavlovic S, Marinkovi D, Tišma M, Gabrovska M, Nikolova D. *Solid green biodiesel catalysts derived from coal fly ash*, in Mansour Al Qubeissi (Ed.). *Renewable Energy - Resources, Challenges and Applications.* London, UK, IntechOpen. 2020; 1-29 https://doi.org/10.5772/intechopen.91703.

[23]   Goh BHH, Chong CT, Ge Y, Ong HC, Ng J-H, Tian B, Ashokkumar V, Lim S, Seljak T, Józsa V. Progress in utilisation of waste cooking oil for sustainable biodiesel and biojet fuel production. *Energy Convers Manage.* 2020; 223: 113296 https://doi.org/10.1016/J.ENCONMAN.2020.113296.

[24]   Jacob A, Ashok B, Alagumalai A, Chyuan OH, Le PTK. Critical review on third generation micro algae biodiesel production and its feasibility as future bioenergy for IC engine applications. *Energy Convers Manage.* 2021; 228: 113655 https://doi.org/10.1016/J.ENCONMAN.2020.113655.

[25]   Perego C, Bosetti A, Ricci M, Millini R. Zeolite Materials for Biomass Conversion to Biofuel. *Energ Fuel.* 2017; 31(8): 7721-7733 https://doi.org/10.1021/ACS.ENERGYFUELS.7B01057.

[26]   Galadima A, Muraza O. Waste materials for production of biodiesel catalysts: Technological status and prospects. *J Clean Prod.* 2020; 263: 121358 https://doi.org/10.1016/J.JCLEPRO.2020.121358.

[27]   Marinković DM, Miladinović MR, Avramović JM, Krstić IB, Stanković MV, Stamenković OS, Jovanović DM, Veljković VB. Kinetic modeling and optimization of sunflower oil methanolysis catalyzed by spherically-shaped CaO/γ-Al$_2$O$_3$ catalyst. *Energy Convers Manage.* 2018; 163: 122-133 https://doi.org/10.1016/J.ENCONMAN.2018.02.048.

[28]   Maghfirah A, Ilmi MM, Fajar ATN, Kadja GTM. A review on the green synthesis of hierarchically porous zeolite. *Mater Today Chem.* 2020; 17: 100348 https://doi.org/10.1016/J.MTCHEM.2020.100348.

[29] Pavlović SM, Marinković DM, Kostić MD, Lončarević DR, Mojović LJV, Stanković MV, Veljković VB. The chicken eggshell calcium oxide ultrasonically dispersed over lignite coal fly ash-based cancrinite zeolite support as a catalyst for biodiesel production. *Fuel.* 2021; 289: 119912 https://doi.org/10.1016/J.FUEL.2020.119912.

[30] Serrano DP, Melero JA, Morales G, Iglesias J, Pizarro P. Progress in the design of zeolite catalysts for biomass conversion into biofuels and bio-based chemicals. *Catal. Rew.* 2018; 60(1): 1-70 https://doi.org/10.1080/01614940.2017.1389109.

[31] Database of Zeolite Structures. http://www.iza-structure.org/databases/. Accessed Apr. 28, 2022.

[32] Colella C, Gualtieri AF. Cronstedt's zeolite. *Microporous Mesoporous Mater.* 2007; 105(3): 213-221 https://doi.org/10.1016/J.MICROMESO.2007.04.056.

[33] Mardiana S, Azhari NJ, Ilmi T, Kadja GTM. Hierarchical zeolite for biomass conversion to biofuel. *Fuel.* 2022; 309: 122119 https://doi.org/10.1016/J.FUEL.2021.122119.

[34] Tschernich RW. *Zeolites of the World*. Phoenix, Arizona 85032: Geoscience Press, Inc., 1992.

[35] Yilmaz B, Müller U. Catalytic applications of zeolites in chemical industry. *Top Catal.* 2009; 52(6-7): 888-895 https://doi.org/10.1007/S11244-009-9226-0/FIGURES/10.

[36] Jiang N, Shang R, Heijman SGJ, Rietveld LC. High-silica zeolites for adsorption of organic micro-pollutants in water treatment. *Water Res.* 2018; 144: 145-161 https://doi.org/10.1016/J.WATRES.2018.07.017.

[37] Li Y, Yu J. Emerging applications of zeolites in catalysis, separation and host-guest assembly. *Nat Rev Mater.* 2021; 6: 12*:* 1156-1174 https://doi.org/10.1038/s41578-021-00347-3.

[38] Scopus - Analyze search results for keyword "biodiesel". https://www.scopus.com/term/analyzer.uri?sid=f1b0ecf09e7389b54b3d1c0a408b6c35&origin=resultslist&src=s&s=TITLE-ABS-KEY%28biodiesel%29&sort=plf-f&sdt=b&sot=b&sl=24&count=45946&analyzeResults=Analyze+results&txGid=54ea8ad5e5d75fc82684a63f1fc06138 Accessed Apr. 28, 2022.

[39] Scopus - Analyze search results for keyword "zeolite + biofuels". https://www.scopus.com/term/analyzer.uri?sid=cc9695bcd8a90aaec9397f592b769798&origin=resultslist&src=s&s=TITLE-ABS-KEY%28zeolite+%2b+biofuels%29&sort=plf-f&sdt=b&sot=b&sl=33&count=875&analyzeResults=Analyze+results&txGid=ffb3d93134573352a7168b2f523ae36a Accessed Apr. 28, 2022.

[40] Zeolites Statistics and Information | U.S. Geological Survey. https://www.usgs.gov/centers/national-minerals-information-center/zeolites-statistics-and-information. Accessed Apr. 28, 2022.

[41] Liu J, Yu J. Toward Greener and Designed Synthesis of Zeolite Materials. *Zeolites Zeolite-like Mater.* 2016; 1-32 https://doi.org/10.1016/B978-0-444-63506-8.00001-X.

[42] Pavlović SM, Marinković DM, Kostić MD, Janković-Častvan IM, Mojović LjV, Stanković MV, Veljković VB*.* A CaO/zeolite-based catalyst obtained from waste chicken eggshell and coal fly ash for biodiesel production. *Fuel.* 2020; 267: 117171 https://doi.org/10.1016/J.FUEL.2020.117171.

[43] Wang Z, Yu J, Xu R. Needs and trends in rational synthesis of zeolitic materials. *Chem Soc Rev.* 2012; 41(5): 1729-1741 https://doi.org/10.1039/C1CS15150A.

[44] Rabie AM, Shaban M, Abukhadra MR, Hosny R, Ahmed SA, Negm NA. Diatomite supported by CaO/MgO nanocomposite as heterogeneous catalyst for biodiesel production from waste cooking oil. *J Mol Liq.* 2019; 279: 224-231 https://doi.org/10.1016/J.MOLLIQ.2019.01.096.

[45] Mohadesi M, Aghel B, Maleki M, Ansari A. The use of KOH/Clinoptilolite catalyst in pilot of microreactor for biodiesel production from waste cooking oil. *Fuel*. 2020; 263: 116659 https://doi.org/10.1016/J.FUEL.2019.116659.

[46] Amalia S, Khalifah SN, Baroroh H, Muiz A, Rahmatullah A, Aini N, Hs MRA, MN Umam, Isnaini IA, Suryana R. Biodiesel production from castor oil using heterogeneous catalyst KOH/zeolite of natural zeolite Bandung Indonesia. *AIP Conf Proc.* 2019; 2120(1): 080016 https://doi.org/10.1063/1.5115754.

[47] Hidayat A, Mukti NIF, Handoko B, Sutrisno B. Biodiesel production from rice bran oil over modified natural zeolite catalyst. *Int J Technol.* 2018; 9(2) 400-411 https://doi.org/10.14716/IJTECH.V9I2.1084.

[48] AbuKhadra MR, Basyouny MG, El-Sherbeeny AM, El-Meligy MA, Abd Elgawad AEE. Transesterification of commercial waste cooking oil into biodiesel over innovative alkali trapped zeolite nanocomposite as green and environmental catalysts. *Sustain Chem Pharm.* 2020; 17: 100289 https://doi.org/10.1016/J.SCP.2020.100289.

[49] Hartono R, Wijanarko A, Hermansyah H. Synthesis of biodiesel using local natural zeolite as heterogeneous anion exchange catalyst. *IOP Conference Series: Mater. Sci Eng.* 2018; 345(1): 012002 https://doi.org/10.1088/1757-899X/345/1/012002.

[50] Fitriana N, Husin H, Yanti D, Pontas K, Alam PN, Ridho M, Iskandar. Synthesis of K2O/Zeolite catalysts by KOH impregnation for biodiesel production from waste frying oil. *IOP Conference Series: Mater Sci Eng.* 2018; 334(1): 012011 https://doi.org/10.1088/1757-899X/334/1/012011.

[51] Taslim, Iriany, Bani O, Parinduri SZDM, Ningsih PRW. Biodiesel production from rice bran oil by transesterification using heterogeneous catalyst natural zeolite modified with K2CO3. *IOP Conference Series: Mater Sci Eng.* 2018; 309(1): 012107 https://doi.org/10.1088/1757-899X/309/1/012107.

[52] Pavlović S, Šelo G, Marinković D, Planinić M, Tišma M, Stanković M. Transesterification of Sunflower Oil over Waste Chicken Eggshell-Based Catalyst in a Microreactor: An Optimization Study. *Micromachines.* 2021; 12(2): 120 https://doi.org/10.3390/MI12020120.

[53] Dianursanti, Delaamira M, Bismo S, Muharam Y. Effect of Reaction Temperature on Biodiesel Production from Chlorella vulgaris using CuO/Zeolite as Heterogeneous Catalyst. *IOP Conference Series: Earth Environ Sci.* 2017; 55(1): 012033 https://doi.org/10.1088/1755-1315/55/1/012033.

[54] Pasae Y, Melawaty L, Ruswanto, Bulo L, Allo EL. Effectiveness of Heterogenous Catalyst In Biodiesel Production Process: The Use of Zeolite, ZnO and Al_2O_3. *J Phys Conf Ser.* 2021; 1899(1): 012032 https://doi.org/10.1088/1742-6596/1899/1/012032.

[55] Otieno SO, Kowenje CO, Okoyo A, Onyango DM, Amisi KO, Nzioka KM. Optimizing production of biodiesel catalysed by chemically tuned natural zeolites. *Mater Today: Proc.* 2018; 5(4): 10561-10569 https://doi.org/10.1016/J.MATPR.2017.12.388.

[56] Mierczynski P, Mosińska M, Szkudlarek L, Chalupka K, Tatsuzawa M, Al Maskari M, Maniukiewicz W, Wahono SK, Vasilev K, Szynkowska-Jozwik, MI. Biodiesel Production on Monometallic Pt, Pd, Ru, and Ag Catalysts Supported on Natural Zeolite. *Materials.* 2020; 14(1): 48 https://doi.org/10.3390/MA14010048.

[57] Alismaeel ZT, Abbas AS, Albayati TM, Doyle AM. Biodiesel from batch and continuous oleic acid esterification using zeolite catalysts. *Fuel.* 2018; 234: 170-176 https://doi.org/10.1016/J.FUEL.2018.07.025.

[58] Marinković DM, Avramović JM, Stanković MV, Stamenković OS, Jovanović DM, Veljković VB. Synthesis and characterization of spherically-shaped $CaO/γ-Al_2O_3$ catalyst and its application in biodiesel production. *Energy Convers Manage.* 2017; 144: 399-413 https://doi.org/10.1016/J.ENCONMAN.2017.04.079.

[59] Mowla O, Kennedy E, Stockenhuber M. In-situ FTIR study on the mechanism of both steps of zeolite-catalysed hydroesterification reaction in the context of biodiesel manufacturing. *Fuel.* 2018; 232: 12-26 https://doi.org/10.1016/J.FUEL.2018.05.096.

[60] Feyzi M, Khajavi G. Investigation of biodiesel production using modified strontium nanocatalysts supported on the ZSM-5 zeolite. *Ind Crops Prod.* 2014; 58: 298-304 https://doi.org/10.1016/J.INDCROP.2014.04.014.

[61] Lawan I, Garba ZN, Zhou W, Zhang M, Yuan Z. Synergies between the microwave reactor and CaO/zeolite catalyst in waste lard biodiesel production. *Renew Energy.* 2020; 145: 2550-2560 https://doi.org/10.1016/J.RENENE.2019.08.008.

[62] Al-Ani A, Mordvinova NE, Lebedev OI, Khodakov AY, Zholobenko V. Ion-exchanged zeolite P as a nanostructured catalyst for biodiesel production. *Energy Rep.* 2019; 5: 357-363 https://doi.org/10.1016/J.EGYR.2019.03.003.

[63] Chen C, Cai L, Zhang L, Fu W, Hong Y, Gao X, Jiang Y, Li L, Yan X, Wu G. Transesterification of rice bran oil to biodiesel using mesoporous NaBeta zeolite-supported molybdenum catalyst: Experimental and kinetic studies. *Chem Eng J.* 2020; 382: 122839 https://doi.org/10.1016/J.CEJ.2019.122839.

[64] Pang H, Yang G, Li L, Yu J. Efficient transesterification over two-dimensional zeolites for sustainable biodiesel production. *Green Energy Environ.* 2020; 5(4): 405-413 https://doi.org/10.1016/J.GEE.2020.10.024.

[65] Purova R, Narasimharao K, Ahmed NSI, Al-Thabaiti S, Al-Shehri A, Mokhtar M, Schwieger W. Pillared HMCM-36 zeolite catalyst for biodiesel production by esterification of palmitic acid. *J Mol Catal A.* 2015; 406: 159-167 https://doi.org/10.1016/J.MOLCATA.2015.06.006.

[66] Yagiz F, Kazan D, Akin AN. Biodiesel production from waste oils by using lipase immobilized on hydrotalcite and zeolites. *Chem Eng J.* 2007; 134(1-3): 262-267 https://doi.org/10.1016/J.CEJ.2007.03.041.

[67] Cheng J, Guo H, Yang X, Mao Y, Qian L, Zhu Y, Yang W. Phosphotungstic acid-modified zeolite imidazolate framework (ZIF-67) as an acid-base bifunctional heterogeneous catalyst for biodiesel production from microalgal lipids, *Energy Convers Manag.* 2021; 232: 113872 https://doi.org/10.1016/J.ENCONMAN.2021.113872.

[68] Fereidooni L, Mehrpooya M. Experimental assessment of electrolysis method in production of biodiesel from waste cooking oil using zeolite/chitosan catalyst with a focus on waste biorefinery. *Energy Convers Manag.* 2017; 147: 145-154 https://doi.org/10.1016/J.ENCONMAN.2017.05.051.

[69] Fereidooni L, Abbaspourrad A, Enayati M. Electrolytic transesterification of waste frying oil using Na+/zeolite-chitosan biocomposite for biodiesel production. *Waste Managt.* 2021; 127: 48-62 https://doi.org/10.1016/J.WASMAN.2021.04.020.

[70] Satriadi H, Pratiwi IY, Khuriyah M, Widayat, Hadiyanto, Prameswari J. Geothermal solid waste derived Ni/Zeolite catalyst for waste cooking oil processing. *Chemosphere.* 2022; 286: 131618 https://doi.org/10.1016/J.CHEMOSPHERE.2021.131618.

[71] Buchori L, Widayat W, Muraza O, Amali MI, Maulida RW, Prameswari J. Effect of Temperature and Concentration of Zeolite Catalysts from Geothermal Solid Waste in Biodiesel Production from Used Cooking Oil by Esterification-Transesterification Process. *Processes.* 2020; 8(12): 1629 https://doi.org/10.3390/PR8121629.

[72] Mahdavianpour M, Pourakbar M, Alavi N, Masihi N, Mirzaei F, Aghayani E. Biodiesel production from waste frying oils in the presence of zeolite synthesized from steel furnace slag. *Inter J Environ Anal Chem.* 2023; 103(4): 814-827 https://doi.org/10.1080/03067319.2020.1863957.

[73] Đặng TH, Chen BH, Lee DJ. Optimization of biodiesel production from transesterification of triolein using zeolite LTA catalysts synthesized from kaolin clay. *J Taiwan Inst Chem.Eng.* 2017; 79: 14-22 https://doi.org/10.1016/J.JTICE.2017.03.009.

[74] Doyle AM, Albayati TM, Abbas AS, Alismaeel ZT. Biodiesel production by esterification of oleic acid over zeolite Y prepared from kaolin. *Renew Energy.* 2016; 97: 19-23 https://doi.org/10.1016/J.RENENE.2016.05.067.

[75] Weitkamp J. Zeolites and catalysis, *Solid State Ion*. 2000; 131(1-2): 175-188. https://doi.org/10.1016/S0167-2738(00)00632-9.

[76] Doyle AM, Alismaeel ZT, Albayati TM, Abbas AS. High purity FAU-type zeolite catalysts from shale rock for biodiesel production. *Fuel.* 2017; 199: 394-402 https://doi.org/10.1016/J.FUEL.2017.02.098.

[77]   Đặng TH, Nguyễn XH, Chou CL, Chen BH. Preparation of cancrinite-type zeolite from diatomaceous earth as transesterification catalysts for biodiesel production. *Renew Energy.* 2021; 174: 347-358 https://doi.org/10.1016/J.RENENE.2021.04.068.

[78]   Murayama N, Yamamoto H, Shibata J. Mechanism of zeolite synthesis from coal fly ash by alkali hydrothermal reaction. *Inter J Miner Process.* 2002; 64(1): 1-17 https://doi.org/10.1016/S0301-7516(01)00046-1.

[79]   Manique MC, Lacerda LV, Alves AK, Bergmann CP. Biodiesel production using coal fly ash-derived sodalite as a heterogeneous catalyst. *Fuel.* 2017; 190: 268-273 https://doi.org/10.1016/J.FUEL.2016.11.016.

[80]   Wang C, Leng S, Guo H, Yu J, Li W, Cao L, Huang J. Quantitative arrangement of Si/Al ratio of natural zeolite using acid treatment. *Appl Surf Sci,* 2019; 498: 143874 https://doi.org/10.1016/J.APSUSC.2019.143874.

[81]   Volli V, Purkait MK. Selective preparation of zeolite X and A from fly ash and its use as catalyst for biodiesel production. *J. Hazard Mater.* 2015; 297: 101-111 https://doi.org/10.1016/J.JHAZMAT.2015.04.066.

[82]   Shabani JM, Babajide O, Oyekola O, Petrik L. Synthesis of Hydroxy Sodalite from Coal Fly Ash for Biodiesel Production from Waste-Derived Maggot Oil. *Catalysts.* 2019; 9: 12: 1052 https://doi.org/10.3390/CATAL9121052.

[83]   Bhandari R, Volli V, Purkait MK. Preparation and characterization of fly ash based mesoporous catalyst for transesterification of soybean oil. *J Environ Cheml Eng.* 2015; 3: 2: 906-914 https://doi.org/10.1016/J.JECE.2015.04.008.

[84]   Go YW, Yeom SH. Fabrication of a solid catalyst using coal fly ash and its utilization for producing biodiesel. *Environ Eng Res.* 2019; 24(2): 324-330 https://doi.org/10.4491/EER.2018.029.

[85]   Li Z, Ding S, Chen C, Qu S, Du L, Lu J, Ding J. Recyclable Li/NaY zeolite as a heterogeneous alkaline catalyst for biodiesel production: Process optimization and kinetics study. *Energy Convers Manage.* 2019; 192: 335-345 https://doi.org/10.1016/J.ENCONMAN.2019.04.053.

[86]   Babajide O, Musyoka N, Petrik L, Ameer F. Novel zeolite Na-X synthesized from fly ash as a heterogeneous catalyst in biodiesel production. *Catal Today.* 2012; 190(1): 54-60 https://doi.org/10.1016/J.CATTOD.2012.04.044.

[87]   He PY, Zhang YJ, Chen H, Han ZC, Liu LC. Low-energy synthesis of kaliophilite catalyst from circulating fluidized bed fly ash for biodiesel production. *Fuel.* 2019; 257: 116041 https://doi.org/10.1016/J.FUEL.2019.116041.

[88]   Lani NS, Ngadi N. Highly efficient CaO-ZSM-5 zeolite/Fe_3O_4 as a magnetic acid-base catalyst upon biodiesel production from used cooking oil. *Appl Nanosci.* 2022; 12: 3755-3769. https://doi.org/10.1007/S13204-021-02121-X

[89]   DIN EN 14214 - European Standards. https://www.en-standard.eu/din-en-14214-liquid-petroleum-products-fatty-acid-methyl-esters-fame-for-use-in-diesel-engines-and-heating-applications-requirements-and-test-methods-includes-amendment-2019/. Accessed Jul. 10, 2022.

[90]   Marinković DM, Stanković MV, Veličković AV, Avramović JM, Cakić MD, Veljković VB. The synthesis of CaO loaded onto Al_2O_3 from calcium acetate and its application in transesterification of the sunflower oil. *Advan Technol.* 2015; 4(1): 26-32 https://doi.org/10.5937/SAVTEH1501026M.

[91]   Standard Specification for Biodiesel Fuel Blend Stock (B100) for Middle Distillate Fuels. https://www.astm.org/d6751-20a.html. Accessed Jul. 10, 2022.

[92]   Patel VR, Dumancas GG, Viswanath LCK, Maples R, Subong BJJ. Castor Oil: Properties, Uses, and Optimization of Processing Parameters in Commercial Production. *Lipid Insights.* 2016; 9: 1-12. https://doi.org/10.4137/LPI.S40233.

[93]   Nikolic D, Seidel C, Felischak M, Milicic T, Kienle A, Seidel-Morgenstern A, Petkovska M. Forced periodic operation of a chemical reactor for methanol synthesis - The search for the best scenario based on Nonlinear Frequency Response Method. Part I Single input modulations. *Chem Eng Sci.* 2022; 248: 117134 https://doi.org/10.1016/j.ces.2021.117134.

[94]   Nikolic D, Seidel C, Felischak M, Milicic T, Kienle A, Seidel-Morgenstern A, Petkovska M. Forced periodic operation of a chemical reactor for methanol synthesis - The search for the best scenario based on Nonlinear Frequency Response Method. Part II Simultaneous modulations of two inputs. Chem Eng Sci. 2022; 248: 117133 https://doi.org/10.1016/j.ces.2021.1171343.

Najnovija saznanja o upotrebi prirodnih zeolita i zeolitnih katalizatora baziranih na otpadu za proizvodnju biodizela

Dalibor M. Marinković i Stefan M. Pavlović

Univerzitet u Beogradu, Institut za hemiju, tehnologiju i metalurgiju, Institut od nacionalnog značaja za Republiku Srbiju, Beograd, Srbija

(Pregledni rad)

Izvod

Imajući u vidu trenutnu svetsku krizu kao i buduće energetske izazove, transformacija biomase u goriva ponovo dobija veliku pažnju zakonodavaca i industrije. Znajući ovo, valorizacija ulja i masnoća putem reakcija transesterifikacije/esterifikacije postaje atraktivan metod za proizvodnju kvalitetnog biodizela pogodnog za postojeće dizel motore. Veliko interesovanje naučnika ukazuje na značajan pomak ka valorizaciji industrijskog otpada kao još jednom pristupu za razvoj ekološki efikasnih procesa. U tom smislu, ovaj rad predstavlja pregled upotrebe zeolitnih katalizatora za dobijanje biogoriva, sa posebnim akcentom na upotrebu otpadnih sirovina u skladu sa principima zelene hemije i održivog razvoja. Zeolitni materijali su veoma pogodni zbog svojih izvanrednih katalitičkih svojstava, uključujući intrinsičke kisele centre, jednostavno nanošenje baznih centara, strukturnu selektivnost i veliku termičku stabilnost. Čisti zeoliti, ili modifikovani nanošenjem aktivnih centara, klasifikovani su u nekoliko grupa u ovom radu u skladu sa njihovim poreklom. Za svaku od različitih grupa zeolita, najrelevantniji skorašnji literaturni rezultati predstavljeni su zajedno sa kritičkim razmatranjem efikasnosti katalizatora, stabilnosti, mogućnosti ponovne upotrebe i ekonomičnosti njihove sinteze. Kao važan deo neophodan za razumevanje i optimizaciju procesa, detaljno su razmotreni mehanizmi reakcije. Na kraju, pažljivo su identifikovani i obrazloženi ključni perspektivni pravci za dalja istraživanja.